Design and Analysis of Multi-antenna and Multi-user

Transmitted Reference Pulse Cluster for Ultra-wideband Communications

by

Congzhi Liu

B. Eng., Shanghai Jiao Tong University, Shanghai, China, 2009

A Thesis Submitted in Partial Fulfillment of the

Requirements for the Degree of

MASTER OF APPLIED SCIENCE

in the Department of Electrical and Computer Engineering

Design and Analysis of Multi-antenna and Multi-user

Transmitted Reference Pulse Cluster for Ultra-wideband Communications

by

Congzhi Liu

B. Eng., Shanghai Jiao Tong University, Shanghai, China, 2009

Supervisory Committee

_____

Dr. Xiaodai Dong, Supervisor

(Department of Electrical and Computer Engineering)

_____

Dr. Lin Cai, Departmental Member

(Department of Electrical and Computer Engineering)

Supervisory Committee

_____

Dr. Xiaodai Dong, Supervisor

(Department of Electrical and Computer Engineering)

_____

Dr. Lin Cai, Departmental Member

(Department of Electrical and Computer Engineering)

ABSTRACT

Antenna diversity for transmitted reference pulse cluster (TRPC) can mitigate the multipath interference and thus greatly improve the BER performance. Different receiver and transmitter diversity schemes have been studied in this thesis, including equal gain combining (EGC), selection combining (SC), delay combining and direct sum. By numerical analysis and simulation, the BER performance of many difference diversity schemes have been compared. For receiver diversity, selection based on simplified log likelihood ratio (SLLR) is the best candicate in terms of implementation complexity and also has the best performance with 2 receivers. For more than 2 receivers, EGC has the best performance at the cost of extra power consumption. For transmitter diversity, selection based on simplified channel quality indicator (SCQI) turns out to be the best choice considering both complexity and performance. In

addition, we have also proposed a new multi-user downlink scheme, pulse pattern TRPC, which shows significant performance gain over time division TRPC.

Contents

List of Figures

ACKNOWLEDGEMENTS

Chapter 1

Introduction

1.1 Ultra-wideband (UWB)

UWB is a wireless technology utilizing a bandwidth larger than 500 MHz or 20% of the center frequency. Fig. 1.1 shows the typical bandwidth of narrowband and UWB systems, in which $f_H - f_L \geq 0.2 f_C$. The development of UWB technology started in the 1960s when Harmuth, Ross, Robins and van Etten led the research in time domain electromagnetics [1]. In the 1972, Ross and Robins invented a sensitive baseband pulse receiver at the Sperry Rand Corporation. Later in 1973, a landmark patent about UWB system design (US patent 3,728,632) was proposed by them [2]. Another significant progress for UWB was published in 1993 by Robert Scholtz who illustrated the multiple access potential of UWB by implementing time-hopping impulse modulation [3]. In 1994, the first low power UWB system was proposed by McEwan which is named as Micropower Impulse Radar (MIR) [4].

The U.S. government has always been an important supporter for UWB commu-
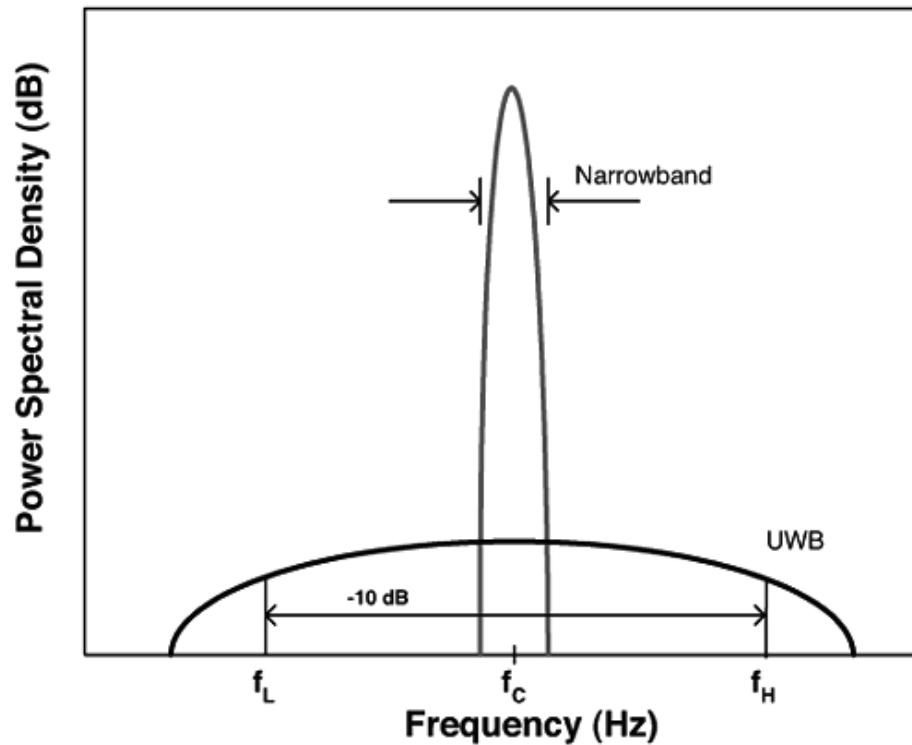
Figure 1.1: The Bandwidth of UWB Communication System [1]

nication. As a matter of fact, the nomenclature ultra wideband was given by the Department of Defense (DOD) to name the communication via impulses. In 2002, the Federal Communications Commission (FCC) in the United States authorized the unlicensed use of frequency 3.1-10.6 GHz which has promoted development of UWB applications [5]. The First Report and Order [6] issued in 2002 categorized UWB systems into three groups, which are communication and measurement systems, vehicular radar systems and imaging systems. Each group was given a different spectral mask and allocated bandwidth. Since there is no restrictions on modulation scheme, a lot of techniques have been proposed, including the combination of Time Hopping (TH), Direct Sequence (DS), Phase Shift Keying (PSK) and Pulse Position Modula-

tion (PPM).

UWB technology has many advantages over conventional narrowband and other alternative systems. First of all, UWB systems can be manufactured with low complexity, which results in low cost, low power consumption and small size. This makes it a great candidate for sensors and hand-held devices. UWB systems also have a large bandwidth which enables high capacity as high as several Gbps [7]. Another important potential factor of UWB systems is security. Since the power of transmitted signal spreads across a large frequency spectrum, UWB signal is noise like. This makes detection and interception of UWB signal very difficult.

There are several areas where have seen rapid development of UWB technologies. The most important area is communication systems, especially short-range wireless communication. Due to its large bandwidth and low cost, UWB may be used widely in sensor networks. For example, it can be used to transmit the information of temperature, blood pressure and medical imaging. In some scenarios, UWB can be a good candidate for devices like mouse, keyboard, smartphones and cars. Another promising area for UWB is position systems. Because of the extremely short duration pulses, UWB can achieve great resolution, sub-centimeter or even sub-millimeter [8], when used for indoor positioning. The extreme short pulses are also immune to some interferences like rain and fog. So UWB antenna arrays can be used to capture both range and angular information in radar systems [9].

The first attempt to standardize UWB is High Date Rate Wireless Personal Area Network (HDR-WPAN) which consider UWB as an ideal candidate for 802.15.3 alternative PHY. There are two competing UWB technologies for the IEEE 802.15.3a task group (TG3a), Direct Sequence (DS) UWB and Multi-Band Orthogonal Frequency

Division Multiplexing (MB-OFDM) UWB. However, the efforts of TG3a failed to achieve 75% majority approval needed for standard in Jan. 2006. Meanwhile, MB-OFDM UWB was approved by ECMA in a PHY and MAC standard (ECMA-368) in Dec. 2005. After that, MB-OFDM UWB was supported and developed by WiMedia Alliance. Another potential candidate, DS-UWB, was adopted by ZigBee Alliance and standardized by IEEE 802.15.4a task group (TG4a). In Aug. 2007, IEEE 802.15.4a was approved and added as an amendment to IEEE 802.15.4 standard [10]. All the channels used in this thesis are generated according to IEEE 802.15.4a channel model [11].

1.2 Transmitted Reference Pulse Cluster (TRPC)

1.2.1 Transmitted Reference (TR)

In a dense multipath environment, the energy of UWB signal is spread over a large amount of multipath components. Rake receiver is implemented to collect these multipath components in conventional UWB systems [12]. As the number of multipath increases, collecting these energy becomes more and more difficult. Transmitted reference (TR) with UWB is introduced to alleviate this problem. The study on TR systems started in the 1950s [13]. In 2002, a delay-hopped TR system was first proposed to be used together with UWB to counter the large amount of multipath components [13]. TR signaling includes data and reference signals separated by a delay T_d. If we denote the data signal as $s_d(t)$, then the reference signal is $s_r(t) = s_d(t - T_d)$. At the

receiver side, the received signal $r(t)$ can be expressed as

$$r(t) = h(t) * [s_d(t) + s_d(t - T_d)] + n(t) \tag{1.1}$$

where $*$ denotes convolution. $h(t)$ is the channel impulse response and $n(t)$ is noise. After that, the receiver can get the decision variable by autocorrelation.

$$D = \int r(t)r^*(t - T_d)dt \tag{1.2}$$

where $r^*(t)$ denotes the complex conjugate of $r(t)$. In order to avoid inter-pulse interference (IPI), T_d should be larger than the length of $h(t)$, which usually ranges from 50 to 200 ns. To perform the autocorrelation, an analog TR receiver needs a delay line with at least T_d long. This is not feasible to implement with available technologies [14]. An alternative solution is a digital receiver. This scheme requires a fast A/D converter with a very high sampling rate, which will consume a lot of power. So this digital solution may not be suitable for some applications due to the high cost and large power consumption [14].

1.2.2   TRPC Scheme

To avoid using long delay lines, a dual pulse structure was proposed in [15], where there are two contiguous pulses in each symbol. Then the delay between data and reference pulses becomes the pulse width T_p, which is feasible to implement in an analog receiver. However, the performance of the DP scheme is poorer than the conventional TR system due to the presence of IPI. To address this problem, a new structure named TRPC was proposed in [16]. In each TRPC symbol, there are N_f

repeated pairs of DPs. All the pulses are closely packed, the required delay line T_d can be as short as the pulse width T_p. The TRPC signal can be expressed as [16]

$$\hat{s}(t) = \sqrt{\frac{E_b}{2N_f}} \sum_{m=-\infty}^{\infty} s(t - mT_s) \tag{1.3}$$

where E_b is the average energy per bit and T_s is the symbol duration. The pulse cluster $s(t)$ for symbol "+1" and "-1" can be given by

$$s(t) = \sum_{i=0}^{N_f-1} g(t - 2iT_d) + b_m g(t - (2i + 1)T_d) \tag{1.4}$$

where $g(t)$ is the convolution results of the transmitter pulse and receiver matched filter. $b_m = +1$ for "+1" symbols and $b_m = -1$ for "-1" symbols.

1.3 Thesis Outline

The main purpose of this thesis is to propose and compare some multi-antenna receiver and transmitter diversity schemes and a multi-user scheme for TRPC. The goal of Chapters 2 and 3 is to find a multi-antenna schemes to improve the BER performance of TRPC and still relatively easy to implement. And Chapter 4 proposes a new multi-user downlink scheme for TRPC. The performance of these schemes is simulated and analyzed in IEEE 802.15.4a UWB channel environments. Based on these results, we have presented the best candidate in terms of performance and complexity.

This thesis is organized as follows.

Chapter 2 introduces equal gain combining (EGC) and several antenna selection criteria for multi-antenna receiver diversity of TRPC. We have shown the results

of simulation and numerical calculation, which indicates that multi-antenna receiver can significantly improve the BER performance. In the 1-by-2 case, selection based on simplified log likelihood ratio (SLLR) is the best candidate in terms of BER performance. But in a system with more than 2 receiver antennas, EGC outperforms all the selection combining schemes.

Chapter 3 proposes several multi-antenna transmitter diversity schemes, including direct sum, delay diversity and selection diversity. Through simulation and numerical analysis, we have shown that the performance gain is not as significant as in receiver diversity schemes. Simplified channel quality indicator (SCQI) has been proved to be the best selection criteria for multi-antenna transmitter schemes and it is also the easiest to implement. We have also studied the case of a 2-by-2 system, which shows that receiver antenna selection based on SLLR and transmitter antenna selection based on SCQI can achieve the best BER performance among all the proposed schemes.

Chapter 4 presents a new multi-user scheme with different pulse patterns. We have proved its performance improvement over time division TRPC through simulation and numerical results. We have proposed pulse patterns for both 2 and 4 users cases. For more than 4 users, we have shown the performance by combining pulse pattern and time division. It yields very good results in both line-of-sight and non-line-of-sight channels and can be easily expanded to support more users as well.

Chapter 5 concludes all the previous chapters.

Chapter 2

Receiver Diversity

2.1 System Model

In wireless communications, signal is transmitted through many different paths, which will result in distortions, phase shifts and time delays. For example, the multipath delays of 802.15.4a UWB channel model 8 [11] can spread larger than 100 ns. In order to mitigate these multipath situations, antenna diversity is especially effective by establishing different links at different antennas. So the probability of getting a reliable link will be greatly increased.

Antenna diversity can be achieved at both the receiver and the transmitter side. We will discuss receiver diversity in this chapter and transmitter diversity in the next chapter. There are three common techniques for receiver diversity: equal gain combining (EGC), selection combining (SC) and maximal ratio combining (MRC). Assume there are N receiver antennas, each antenna is given a different weight w_i to form the output signal. All the weights are the same for EGC. If SC is applied,
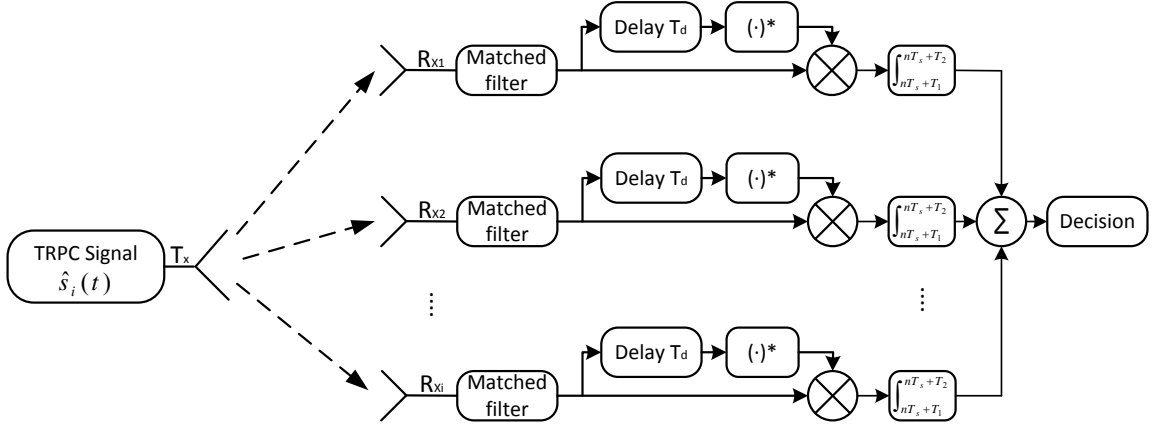
Figure 2.1: one transmitter antenna and multiple receiver antennas with EGC

one of the chosen weight will be 1 and all the others will be 0. And MRC obtains the weight that maximizes the output SNR which makes it the optimal technique in terms of SNR for conventional receiver diversity. However it requires channel state information at receiver which is not present for non-coherent detection schemes such as TRPC. So MRC cannot be applied to TRPC. We will only discuss EGC and SC in this chapter.

2.1.1 Equal Gain Combining

In this section, we consider a system with single transmit antenna and multiple receive antennas (SIMO). The schematic diagram for the SIMO system is shown in Fig. 2.1. The TRPC pulse structure here is the same as in [16]. There are N_f reference pulses and N_f data pulses in each pulse cluster. The TRPC signal $\hat{s}_i(t)$ in Fig. 2.1 can be expressed as

$$\hat{s}(t) = \sqrt{\frac{E_b}{2N_f}} \sum_{m=-\infty}^{\infty} s(t - mT_s) \tag{2.1}$$

where T_s is the symbol duration and $s(t)$ is the pulse cluster which is illustrated in (1.4). And the channel experienced by each receiver antenna is independent from one another. According to [11], the UWB channels can be modelled as

$$h(t) = \sum_{l=0}^{L-1} \alpha_l \delta(t - \tau_l) \tag{2.2}$$

where $h(t)$ is the impulse response of the channel. L, α_l and τ_l denotes the number of multipath, the amplitude and delay of lth multipath delay respectively.

Then the received signal $r_i(t)$ at the ith receiver will be the convolution of $\hat{s}(t)$ and $h_i(t)$ plus noise $n(t)$,

$$r_i(t) = \hat{s}(t) * h_i(t) + n(t). \tag{2.3}$$

The received signal becomes $\hat{r}_i(t)$ after the matched filter. Then we have the decision variable (DV) after the output of auto-correlation

$$D_i = \int_{nT_s+T_1}^{nT_s+T_2} \hat{r}_i(t)\hat{r}_i^*(t - T_d)dt \tag{2.4}$$

After equal gain combining (EGC), which is adding all the receivers' DV for decision, we have

$$D_{EGC} = \sum_{i=1}^{N} D_i = \sum_{i=1}^{N} \int_{nT_s+T_1}^{nT_s+T_2} \hat{r}_i(t)\hat{r}_i^*(t - T_d)dt \tag{2.5}$$

where N is the number of receivers.

According to [16], each D_i can be approximated by a Gaussian random variable. So D_{EGC} can also be approximated as a Gaussian random variable and the mean of

$\text{Re}\{D_{EGC}\}$ can be given by

$$
\begin{aligned}
\mu &= \text{E}[\text{Re}\{D_{EGC}\}] \\
&= \sum_{i=1}^{N} \text{E}[\text{Re}\{D_i\}]
\end{aligned}
\tag{2.6}
$$

And the variance of $\text{Re}\{D_{EGC}\}$ can be approximated by $\sum \sigma_{D_i}^2$.

If zero decision threshold (ZDT) is applied, $\text{Re}\{D_{EGC}\}$ will be compared with zero to make the decision. Otherwise if we adopt adaptive decision threshold (ADT) [17], $\text{Re}\{D_{EGC}\}$ will be compared with ξ_{EGC} which is estimated by a training process. First we send a training sequence consisting of '+1' and '-1' symbols in turn. The total length of the sequence is N_t, so there will be $\frac{1}{2}N_t$ '+1' and '-1' symbols respectively. If $D_{i,m}$ is the mth DV at the ith receiver. we have

$$
\hat{\xi}_{EGC} = \text{Re}\{\frac{1}{N_t} \sum_{i=1}^{N} \sum_{m=1}^{N_t} D_{i,m}\}
\tag{2.7}
$$

Then we compare $\text{Re}\{D_{EGC}\}$ with $\hat{\xi}_{EGC}$ to make decisions.

2.1.2   Selection Combining

In this section, we present several antenna selection criteria. Numerical analysis and simulations about them are showed later in order to decide which one is the best criteria. The system model is similar to that of EGC, except that the final DV is selected from one of the DVs from different receiver antennas, as shown in Fig. 2.2. This selection process can be done symbol by symbol, if we apply certain criteria such as DV, NCQI, LLR or SLLR. Otherwise it can be done once every packet, when
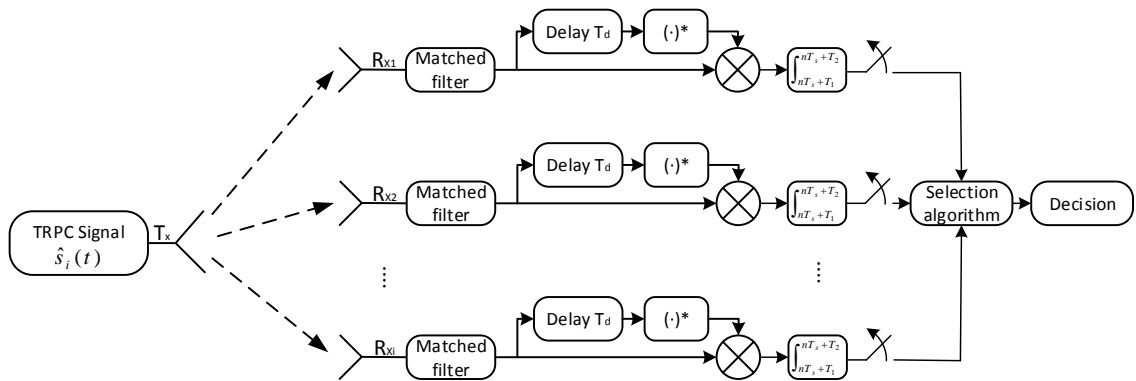
Figure 2.2: one transmitter antenna and multiple receiver antennas with selection combining

channel length, received energy or average received power is used as the selection criteria.

1. Selection Based on Decision Variable

    If we apply ZDT, then the DV with the largest absolute value is selected. And antenna $R_{Xi_{SC\_DV}}$ is considered to be the best one. This selection is performed once for each symbol.

$$i_{SC\_DV} = \operatorname*{argmax}_{i} (|D_{i,n}|) \tag{2.8}$$

    where $D_{i,n}$ is the nth DV at the ith receiver. If ADT is applied, similarly we have

$$i_{SC\_DV} = \operatorname*{argmax}_{i} (|D_{i,n} - \hat{\xi}_i|) \tag{2.9}$$

2. Selection Based on Channel Length

    When the channel impulse response (CIR) first exceeds a certain threshold, we mark that as the start point of CIR. And the end point of the CIR is when the CIR falls below the threshold for the last time. We call the length in between the start and end points as the channel length.

    Typically, a shorter channel length means less noise energy is collected while collecting enough signal energy, which results in a better BER performance . So we selected the receive antenna with the shortest channel length as the best one.

If the start and end points for the ith CIR are $t_s(i)$ and $t_e(i)$ respectively, then the selected receiver antenna index will be

$$i_{SC\_CL} = \operatorname*{argmin}_{i} \left(t_e(i) - t_s(i)\right) \tag{2.10}$$

3. Selection Based on Received Energy

Here, the received energy is defined as the signal energy within the significant part of the received signal. The start and end points of the significant part are acquired according to the CIR.

$$RE_i = \int_{t_s(i)}^{t_e(i)} |r_i(t)|^2 \, dt \tag{2.11}$$

Then the selected receive antenna index will be,

$$i_{SC\_RE} = \operatorname*{argmax}_{i} \left(\int_{t_s(i)}^{t_e(i)} |r_i(t)|^2 dt\right) \tag{2.12}$$

4. Selection Based on Average Received Power

The average received power is defined as the average signal power over the region of the significant part of the received signal.

$$ARP_i = \frac{\int_{t_s(i)}^{t_e(i)} |r_i(t)|^2 dt}{t_e(i) - t_s(i)} \tag{2.13}$$

So the selected receive antenna index is,

$$i_{SC\_ARE} = \operatorname*{argmax}_{i} \left(\frac{\int_{t_s(i)}^{t_e(i)} |r_i(t)|^2 dt}{t_e(i) - t_s(i)} \right) \tag{2.14}$$

5. Selection Based on Normalized Channel Quality Indicator (NCQI)

NCQI can be considered as a weighted adaptive threshold. The weight E_i is defined as $E_i = \frac{1}{2} \{m_i(+1) - m_i(-1)\}$, which normalizes the distance between $D_{i,n}$ and $\hat{\xi}_i$.

$$NCQI_i = \frac{\left| D_{i,n} - \hat{\xi}_i \right|}{E_i} \tag{2.15}$$

And the antenna index with largest NCQI is selected for each symbol

$$i_{SC\_NCQI} = \operatorname*{argmax}_{i} \left(\frac{\left| D_{i,n} - \hat{\xi}_i \right|}{E_i} \right) \tag{2.16}$$

6. Selection Based on Log Likelihood Ratio (LLR)

The likelihood ratio is the probability for a single bit to be $\hat{b}_i$ over the probability for it to be $-\hat{b}_i$. And LLR is defined as the natural logarithm of this ratio.

$$
LLR_i = \ln \left[\frac{\frac{1}{\sqrt{2\pi}\sigma_i(\hat{b}_i)} e^{-\frac{\left(D_{i,n} - m_i(\hat{b}_i)\right)^2}{2\sigma_i^2(\hat{b}_i)}}}{\frac{1}{\sqrt{2\pi}\sigma_i(-\hat{b}_i)} e^{-\frac{\left(D_{i,n} - m_i(-\hat{b}_i)\right)^2}{2\sigma_i^2(-\hat{b}_i)}}} \right]
$$
$$
= \ln \left[\frac{\sigma_i\left(-\hat{b}_i\right)}{\sigma_i\left(\hat{b}_i\right)} \right] + \frac{\left[D_{i,n} - m_i\left(-\hat{b}_i\right)\right]^2}{2\sigma_i^2\left(-\hat{b}_i\right)} - \frac{\left[D_{i,n} - m_i\left(\hat{b}_i\right)\right]^2}{2\sigma_i^2\left(\hat{b}_i\right)} \tag{2.17}
$$

Here, $\hat{b}_{i,n}$ is the nth decoded bit ($+1$ or -1) at the ith receiver antenna. And the selected antenna index is

$$i_{SC\_LLR} = \underset{i}{\text{argmax}}\left(LLR_i\right) \tag{2.18}$$

7. Selection Based on Simplified Log Likelihood Ratio (SLLR)

Since $\sigma_i\left(+1\right) \approx \sigma_i\left(-1\right)$, we can simplify LLR as follows,

$$
\begin{aligned}
LLR_i &\approx 0 + \frac{\left[-2m_i\left(-\hat{b}_i\right) + 2m_i\left(\hat{b}_i\right)\right] D_{i,n} + \left[m_i\left(-\hat{b}_i\right)^2 - m_i\left(\hat{b}_i\right)^2\right]}{2\sigma_i^2} \\
&= \frac{\left[m_i\left(\hat{b}_i\right) - m_i\left(-\hat{b}_i\right)\right]\left[2D_{i,n} - m_i\left(\hat{b}_i\right) - m_i\left(-\hat{b}_i\right)\right]}{2\sigma_i^2} \\
&= \frac{\left[m_i\left(\hat{b}_i\right) - m_i\left(-\hat{b}_i\right)\right]\left[D_{i,n} - \hat{\xi}_i\right]}{\sigma_i^2} \\
&= \begin{cases} \frac{2E_i(D_{i,n}-\hat{\xi}_i)}{\sigma_i^2} & \hat{b}_i = +1 \\ \frac{-2E_i(D_{i,n}-\hat{\xi}_i)}{\sigma_i^2} & \hat{b}_i = -1 \end{cases} \\
&= \frac{2E_i\left|D_{i,n} - \hat{\xi}_i\right|}{\sigma_i^2}
\end{aligned}
\tag{2.19}
$$

So the index of the selected antenna will be,

$$i_{SC\_SLLR} = \underset{i}{\text{argmax}}\left(\frac{2E_i\left|D_{i,n} - \hat{\xi}_i\right|}{\sigma_i^2}\right) \tag{2.20}$$

2.2   Numerical Analysis

2.2.1   Equal gain combining

According to [16], the decision variable in TRPC can be approximated as a Gaussian RV and expressed as

$$D = D_1 + D_2 + D_3 + D_4$$

$$D_1 = \frac{E_b}{2N_f} \int_{T_1}^{T_2} q\left(t\right) q^*\left(t - T_d\right) dt$$

$$D_2 = \sqrt{\frac{E_b}{2N_f}} \int_{T_1}^{T_2} q\left(t\right) n^*\left(t - T_d\right) dt \qquad (2.21)$$

$$D_3 = \sqrt{\frac{E_b}{2N_f}} \int_{T_1}^{T_2} q^*\left(t - T_d\right) n\left(t\right) dt$$

$$D_4 = \int_{T_1}^{T_2} n\left(t\right) n^*\left(t - T_d\right) dt$$

It is already shown in [16] that $E[\mathrm{Re}\{D\}] \approx \mathrm{Re}\{D_1\}$ and $\mathrm{Var}[\mathrm{Re}\{D\}] = \mathrm{Var}[\mathrm{Re}\{D_2 + D_3\}] + \mathrm{Var}[\mathrm{Re}\{D_4\}]$

If we have N receiver antennas, and equal gain combining is applied. The decision variable after combining will be $D_{EGC} = \sum_{i=1}^{N} D_i$. Since each receiver antenna is independent, the combined variance will be the sum of the variances of all the branches.

$$\sigma_{D_{EGC}}^2 = \sum_{i=1}^{N} \sigma_{D_i}^2 \qquad (2.22)$$

Since D can be closely approximated as a Gaussian RV, we can easily derive the probability of error for EGC. When ZDT is utilized and data bit is $+1$,

$$Pe|_{zdt,+1} = \frac{1}{2}\left[1 + \text{erf}\left(\frac{0 - \mu_{D_{EGC}}}{\sqrt{2\sigma_{D_{EGC}}^2}}\right)\right] \tag{2.23}$$

Similarly we have

$$Pe|_{zdt,-1} = \frac{1}{2}\left[1 - \text{erf}\left(\frac{0 - \mu_{D_{EGC}}}{\sqrt{2\sigma_{D_{EGC}}^2}}\right)\right] \tag{2.24}$$

$$Pe|_{adt,+1} = \frac{1}{2}\left[1 + \text{erf}\left(\frac{\xi - \mu_{D_{EGC}}}{\sqrt{2\sigma_{D_{EGC}}^2}}\right)\right] \tag{2.25}$$

$$Pe|_{adt,-1} = \frac{1}{2}\left[1 - \text{erf}\left(\frac{\xi - \mu_{D_{EGC}}}{\sqrt{2\sigma_{D_{EGC}}^2}}\right)\right] \tag{2.26}$$

Therefore the probability of error for EGC will be $Pe = \frac{1}{2}Pe|_{+1} + \frac{1}{2}Pe|_{-1}$ for both ZDT and ADT.

2.2.2   Selection Based on Decision Variable

If ZDT is applied, the index of the selected receiver antenna for the nth symbol is

$$i_{SC\_DV} = \arg\max_i\left(|D_{i,n}|\right) \tag{2.27}$$

In the following derivations, we denote $D_{i,n}$ as D_i for notation simplicity since only the nth symbol is considered here. The moment generating function (MGF) of D is

given by

$$
\begin{aligned}
M_D(s) &= \mathbb{E}\left[e^{sD}\right] \\
&= \mathbb{E}\left[\exp\left(s\sum_{i=1}^{N}T(D_i)\right)\right], \quad s \in \mathbb{R}
\end{aligned}
\tag{2.28}
$$

where $\mathbb{E}$ denotes expectation and $T(D_i)$ is the testing function

$$
T(D_i) = \begin{cases} D_i & \text{if } i = i_{SC\_DV} \\ 0 & \text{otherwise} \end{cases}
\tag{2.29}
$$

If we denote $f_i(D)$ as the probability density function of D_i and $F_i(D)$ as the cumulative distribution function of D_i. For a given D, it can come from any of the N receivers. If i_{SC_DV} is fixed, there are $(N-1)!$ possible sorted sequences for the rest $N-1$ receivers. And for any $j \neq i_{SC\_DV}$, $-|D_{i_{SC\_DV}}| \leq |D_j| \leq |D_{i_{SC\_DV}}|$. So we have

$$
\begin{aligned}
M_D(s) &= \sum_{i=1}^{N}\int_{-\infty}^{\infty}\sum_{(N-1)!}\int\int\cdots\int e^{sD}f_i(D)f_{j_1}(D_{j_1})\cdots \\
&\quad f_{j_{N-1}}(D_{j_{N-1}})\,dD_{j_1}\cdots dD_{j_{N-1}}dD \\
&= \sum_{i=1}^{N}\int_{-\infty}^{\infty}e^{sD}f_i(D)\sum_{(N-1)!}\int_{-|D|}^{|D|}f_{j_1}(D_{j_1})\,dD_{j_1}\cdots \\
&\quad \int_{-|D_i|}^{|D_i|}f_{j_{N-1}}(D_{j_{N-1}})\,dD_{j_{N-1}}dD \\
&= \sum_{i=1}^{N}\int_{-\infty}^{\infty}e^{sD}f_i(D)\left(\sum_{(N-1)!}\prod_{j=j_1}^{j_{N-1}}\int_{-|D|}^{|D|}f_j(D_j)\,dD_j\right)dD \\
&= \sum_{i=1}^{N}\int_{-\infty}^{\infty}e^{sD}f_i(D)\left(\sum_{(N-1)!}\prod_{j=j_1}^{j_{N-1}}(F_j(|D|)-F_j(-|D|))\right)dD, \quad j \neq i
\end{aligned}
\tag{2.30}
$$

Given the definition of MGF,

$$M_D(s) = \int_{-\infty}^{\infty} e^{sD} f_D(D) \mathrm{d}D \tag{2.31}$$

From (2.30) and (2.31), we can see that

$$f_D(D) = \sum_{i=1}^{N} f_i(D) \sum_{(N-1)!} \prod_{j=j_1}^{j_{N-1}} (F_j(|D|) - F_j(-|D|)), \quad j \neq i \tag{2.32}$$

We can further simplify it if there are only two receiver antennas $(N = 2)$,

$$
\begin{aligned}
f_D(D) &= \sum_{i=1}^{2} f_i(D) \left[F_j(|D|) - F_j(-|D|) \right], \quad j \in \{1, 2\}, j \neq i \\
&= \sum_{i=1}^{2} f_i(D) \left[\frac{1}{2} \mathrm{erf}\left(\frac{|D| - \mu_j}{\sqrt{2\sigma_j^2}} \right) - \frac{1}{2} \mathrm{erf}\left(\frac{-|D| - \mu_j}{\sqrt{2\sigma_j^2}} \right) \right]
\end{aligned} \tag{2.33}
$$

where $f_i(D) = \frac{1}{\sqrt{2\pi\sigma_i^2}} \exp\left(\frac{-(D-\mu_i)^2}{2\sigma_i^2} \right)$, so the probability of error is

$$Pe = \frac{1}{2} \int_{-\infty}^{0} f_D(D)|_{data=+1} \mathrm{d}D + \frac{1}{2} \int_{0}^{+\infty} f_D(D)|_{data=-1} \mathrm{d}D \tag{2.34}$$

$$f_D(D)|_{data=+1} = \frac{1}{\sqrt{2\pi\sigma_1^2}} \exp\left(\frac{-(D-\mu_1)^2}{2\sigma_1^2}\right) \left[\frac{1}{2}\text{erf}\left(\frac{-D-\mu_2}{\sqrt{2\sigma_2^2}}\right) - \frac{1}{2}\text{erf}\left(\frac{D-\mu_2}{\sqrt{2\sigma_2^2}}\right)\right]$$

$$+ \frac{1}{\sqrt{2\pi\sigma_2^2}} \exp\left(\frac{-(D-\mu_2)^2}{2\sigma_2^2}\right) \left[\frac{1}{2}\text{erf}\left(\frac{-D-\mu_1}{\sqrt{2\sigma_1^2}}\right) - \frac{1}{2}\text{erf}\left(\frac{D-\mu_1}{\sqrt{2\sigma_1^2}}\right)\right]$$

$$f_D(D)|_{data=-1} = \frac{1}{\sqrt{2\pi\sigma_1^2}} \exp\left(\frac{-(D-\mu_1)^2}{2\sigma_1^2}\right) \left[\frac{1}{2}\text{erf}\left(\frac{D-\mu_2}{\sqrt{2\sigma_2^2}}\right) - \frac{1}{2}\text{erf}\left(\frac{-D-\mu_2}{\sqrt{2\sigma_2^2}}\right)\right]$$

$$+ \frac{1}{\sqrt{2\pi\sigma_2^2}} \exp\left(\frac{-(D-\mu_2)^2}{2\sigma_2^2}\right) \left[\frac{1}{2}\text{erf}\left(\frac{D-\mu_1}{\sqrt{2\sigma_1^2}}\right) - \frac{1}{2}\text{erf}\left(\frac{-D-\mu_1}{\sqrt{2\sigma_1^2}}\right)\right]$$

$$(2.35)$$

If ADT is applied, we need to find $i_{SC\_DV} = \arg\max_i\left(\left|D_i - \hat{\xi}_i\right|\right)$. We can denote $\hat{D}_i = D_i - \hat{\xi}_i$, then the derivation is the same as ZDT by replacing D with $\hat{D}$ in (2.28)-(2.35).

2.2.3 Selection Based on Normalized Channel Quality Indicator (NCQI)

We denote $\hat{D}_i = D_i - \hat{\xi}_i$, and NCQI can be expressed as

$$NCQI_i = \frac{\left|\hat{D}_i\right|}{E_i} \tag{2.36}$$

So the selected antenna index will be

$$i_{SC\_NCQI} = \arg\max_i\left(\frac{\left|\hat{D}_i\right|}{E_i}\right) \tag{2.37}$$

Similar to (2.28)-(2.35), we have the MGF for NCQI

$$M_{\hat{D}}(s) = \sum_{i=1}^{N} \int_{-\infty}^{\infty} e^{s\hat{D}} f_i\left(\hat{D}\right) \left(\sum \frac{j_{N-1}}{(N-1)!} \prod_{j=j_1} \left(F_j\left(U_{\hat{D}_j}\right) - F_j\left(L_{\hat{D}_j}\right) \right) \right) \mathrm{d}\hat{D}, \quad j \neq i$$

$$(2.38)$$

where $U_{\hat{D}_j}$ and $L_{\hat{D}_j}$ represent the upper bound and lower bound of $\hat{D}_j$. From the definition of NCQI, if $NCQI_j < NCQI_i$, then $-\frac{E_j}{E_i}\left|\hat{D}_i\right| < \hat{D}_j < \frac{E_j}{E_i}\left|\hat{D}_i\right|$. So $L_{\hat{D}_j} = -\frac{E_j}{E_i}\left|\hat{D}_i\right|$ and $U_{\hat{D}_j} = \frac{E_j}{E_i}\left|\hat{D}_i\right|$.

From (2.38) we have the PDF of $\hat{D}$

$$f_{\hat{D}}(\hat{D}) = \sum_{i=1}^{N} f_i\left(\hat{D}\right) \left(\sum \frac{j_{N-1}}{(N-1)!} \prod_{j=j_1} \left(F_j\left(U_{\hat{D}_j}\right) - F_j\left(L_{\hat{D}_j}\right) \right) \right) \mathrm{d}\hat{D}, \quad j \neq i \qquad (2.39)$$

Consider the scenario with two receivers ($N = 2$),

$$f_{\hat{D}}\left(\hat{D}\right) = \sum_{i=1}^{2} f_i\left(\hat{D}\right) \left[F_j\left(U_{\hat{D}_j}\right) - F_j\left(L_{\hat{D}_j}\right) \right], \quad j \in \{1,2\}, j \neq i$$

$$= \sum_{i=1}^{2} f_i\left(\hat{D}\right) \left[\frac{1}{2}\mathrm{erf}\left(\frac{\frac{E_j}{E_i}\left|\hat{D}\right| - \mu_j}{\sqrt{2\sigma_j^2}} \right) - \frac{1}{2}\mathrm{erf}\left(\frac{-\frac{E_j}{E_i}\left|\hat{D}\right| - \mu_j}{\sqrt{2\sigma_j^2}} \right) \right]$$

$$= \frac{1}{\sqrt{2\pi\sigma_1^2}} \exp\left(\frac{-\left(\hat{D}-\mu_1\right)^2}{2\sigma_1^2} \right) \left[\frac{1}{2}\mathrm{erf}\left(\frac{\frac{E_2}{E_1}\left|\hat{D}\right| - \mu_2}{\sqrt{2\sigma_2^2}} \right) - \frac{1}{2}\mathrm{erf}\left(\frac{-\frac{E_2}{E_1}\left|\hat{D}\right| - \mu_2}{\sqrt{2\sigma_2^2}} \right) \right]$$

$$+ \frac{1}{\sqrt{2\pi\sigma_2^2}} \exp\left(\frac{-\left(\hat{D}-\mu_2\right)^2}{2\sigma_2^2} \right) \left[\frac{1}{2}\mathrm{erf}\left(\frac{\frac{E_1}{E_2}\left|\hat{D}\right| - \mu_1}{\sqrt{2\sigma_1^2}} \right) - \frac{1}{2}\mathrm{erf}\left(\frac{-\frac{E_1}{E_2}\left|\hat{D}\right| - \mu_1}{\sqrt{2\sigma_1^2}} \right) \right]$$

$$(2.40)$$

where $\mu_i = \operatorname{Re}\{D\} - \hat{\xi}_i$. The bit error rate will be

$$Pe = \frac{1}{2}\int_{-\infty}^{0} f_{\hat{D}}\left(\hat{D}\right)\Big|_{data=+1} \mathrm{d}\hat{D} + \frac{1}{2}\int_{0}^{+\infty} f_{\hat{D}}\left(\hat{D}\right)\Big|_{data=-1} \mathrm{d}\hat{D} \qquad (2.41)$$

2.2.4 Selection Based on Simplified Log Likelihood Ratio (SLLR)

For selection based on LLR, there is no closed form expression for $U_{\hat{D}_j}$ or $L_{\hat{D}_j}$ in the MGF. But we can approximate it by SLLR. The index of the selected receiver antenna based on SLLR is

$$i_{SC\_SLLR} = \operatorname*{argmax}_{i}\left(\frac{2E_i\left|D_i - \hat{\xi}_i\right|}{\sigma_i^2}\right) \qquad (2.42)$$

$f_{\hat{D}}\left(\hat{D}\right)$ will be the same as in (2.39). The only difference here is the $U_{\hat{D}_j}$ and $L_{\hat{D}_j}$. From (2.42), if $SLLR_j < SLLR_i$, we can get $-\frac{\sigma_j^2}{\sigma_i^2}\frac{E_i}{E_j}\left|\hat{D}_i\right| < \hat{D}_j < \frac{\sigma_j^2}{\sigma_i^2}\frac{E_i}{E_j}\left|\hat{D}_i\right|$. So we can write the PDF of $\hat{D}$ when $N = 2$ as

$$f_{\hat{D}}\left(\hat{D}\right) = \sum_{i=1}^{2} f_i\left(\hat{D}\right) \left[\frac{1}{2}\text{erf}\left(\frac{\frac{\sigma_j^2}{\sigma_i^2}\frac{E_i}{E_j}\left|\hat{D}\right| - \mu_j}{\sqrt{2\sigma_j^2}}\right) - \frac{1}{2}\text{erf}\left(\frac{-\frac{\sigma_j^2}{\sigma_i^2}\frac{E_i}{E_j}\left|\hat{D}\right| - \mu_j}{\sqrt{2\sigma_j^2}}\right)\right], \quad j \neq i$$

$$= \frac{1}{\sqrt{2\pi\sigma_1^2}}\exp\left(\frac{-\left(\hat{D} - \mu_1\right)^2}{2\sigma_1^2}\right) \left[\frac{1}{2}\text{erf}\left(\frac{\frac{\sigma_2^2}{\sigma_1^2}\frac{E_1}{E_2}\left|\hat{D}\right| - \mu_2}{\sqrt{2\sigma_2^2}}\right) - \frac{1}{2}\text{erf}\left(\frac{-\frac{\sigma_2^2}{\sigma_1^2}\frac{E_1}{E_2}\left|\hat{D}\right| - \mu_2}{\sqrt{2\sigma_2^2}}\right)\right]$$

$$+ \frac{1}{\sqrt{2\pi\sigma_2^2}}\exp\left(\frac{-\left(\hat{D} - \mu_2\right)^2}{2\sigma_2^2}\right) \left[\frac{1}{2}\text{erf}\left(\frac{\frac{\sigma_1^2}{\sigma_2^2}\frac{E_2}{E_1}\left|\hat{D}\right| - \mu_1}{\sqrt{2\sigma_1^2}}\right) - \frac{1}{2}\text{erf}\left(\frac{-\frac{\sigma_1^2}{\sigma_2^2}\frac{E_2}{E_1}\left|\hat{D}\right| - \mu_1}{\sqrt{2\sigma_1^2}}\right)\right]$$

$$(2.43)$$

The bit error rate can be calculated using

$$Pe = \frac{1}{2}\int_{-\infty}^{0} f_{\hat{D}}\left(\hat{D}\right)\Big|_{data=+1} \mathrm{d}\hat{D} + \frac{1}{2}\int_{0}^{+\infty} f_{\hat{D}}\left(\hat{D}\right)\Big|_{data=-1} \mathrm{d}\hat{D} \qquad (2.44)$$

2.3 Simulation and Numerical Results for Receiver Diversity

In this section, we will show the simulation and numerical results in a TRPC SIMO system. All the simulations in this thesis are done in MATLAB. The channel models used here are CM1 and CM8 in IEEE 802.15.4a channel model [11]. CM1 is based on measurements in residential line-of-sight (LOS) environments, which has a strong first tap and limited multipath[11]. While CM8 represents industrial Non-LOS (NLOS) environments with a very large delay spread. A root-raised-cosine (RRC) filter with a roll-off factor $\beta = 0.25$ is used on both transmitter side and receiver side. Pulse

width of the RRC pulse T_p is 2.02 ns. The data rate $b_r = 4$ Mbps, symbol duration $T_s = 250$ ns, number of repetition in one TRPC symbol $N_r = 4$, sampling rate $f_s = 3952$ MHz, scale factor used to determine the integration interval $s = 0.3$.

Fig. 2.3 shows the simulation results of BER performance when EGC is used in receiver diversity. The length of training sequence is $N_t = 32$ for the ADT part in the simulation. If ADT is applied, 1-by-2 system outperforms 1-by-1 by about 3 dB at BER=10^{-5}, 1-by-3 outperforms 1-by-2 by 1.5 dB and 1-by-4 outperforms 1-by-3 by 1 dB. This indicates that the performance gain introduced by each additional receiver antenna is getting smaller as the number of receiver antenna increases. So it is a trade-off between hardware complexity and performance gain in implementations. In real implementations, power consumption and hardware cost are important factors for UWB receivers. So two receiver antennas should be a good balance. Moreover, the BER gaps between ZDT and ADT is smaller with more receiver antennas. The data rate of ZDT implementation will be slightly larger than that of ADT since ADT needs additional training overhead. For 1-by-4 system, the gap between ZDT and ADT is about 0.3 dB. Such a small gap is likely to be offset by training overhead and hardware complexity of ADT implementation. In that case, ZDT is a viable option for multiple receiver antennas. Fig. 2.4 represents the simulation results of BER performance of EGC in CM8 channels. At BER $= 10^{-5}$, the performance improvement of each additional receiver antenna is 2.2 dB, 1.2 dB and 0.8 dB respectively. These performance gaps are slightly smaller than that of CM1. Besides, the gaps between ZDT and ADT are smaller than that of CM1 as well.

Fig. 2.5 and Fig. 2.6 show the BER performance for different antenna selection criteria introduced in Section 2.1 when there are 2 receiver antennas in the system.

From Fig. 2.5, we can see that EGC and antenna selection based on DV significantly outperform selection based on channel length, received energy and average received power. And Fig. 2.6 shows that the performance of EGC, selection based on DV, NCQI, LLR and SLLR are very close if ADT is adopted. So in the rest of this thesis, we will not consider receiver selection base on channel length, received energy or average received power.

Fig. 2.7 and Fig. 2.8 represent the comparison between numerical and simulation results with EGC and antenna selection criteria in CM1 and CM8 channels when there are 2 receiver antennas in the system. As we can see, there is very little difference between numerical and simulation results. The performance of EGC and selection based on DV are almost the same with both ZDT and ADT. Among all the selection criteria considered, SLLR performs slightly better than the others and NCQI performs the worst. Since the implementation complexity of SLLR is acceptable, so SLLR should be our choice among EGC and all the selection criteria for 1-by-2 system.

Fig. 2.9 shows the simulation results of receiver diversity with more than 2 receiver antennas in CM1 channels. For a fair comparison, all the results are obtained using ADT. Antenna selection based on DV and SLLR have similar performance in all the systems. In 1-by-2 system, the performance of EGC and antenna selection are almost the same. But in 1-by-3 and 1-by-4 systems, EGC has performance improvement of 0.5 dB and 0.8 dB over antenna selection at BER $= 10^{-5}$. So in a system with more than 2 receiver antennas, EGC has the best BER performance among all the schemes we have considered. However, from the implementation perspective, all the antennas have to work at the same time for EGC, which means more energy consumption for the receiver. While antenna selection schemes can be simplified to perform selection

once for every data packet. In this way, the index of the selected antenna can be chosen based on the training sequence. Therefore only one antenna will be operating during the data packet, which means much less energy consumption. This may be an important factor when designing a low power receiver. The BER performance of receiver diversity with more than 2 receiver antennas in CM8 channels is illustrated in Fig. 2.10. EGC still has the best BER performance in CM8 channels but the performance gaps are smaller. EGC outperforms antenna selection by 0.3 dB and 0.6 dB in 1-by-3 and 1-by-4 systems.

2.4   Summary

In this chapter, several receiver antenna selection criteria have been proposed and compared with EGC. Through numerical calculation and simulation, we have showed that selection based on SLLR has the best BER performance among all the selection criteria. And it is slightly better in 1-by-2 case. However, in a system with more than 2 receiver antennas, EGC achieves a significant performance gain over all the other schemes.

Figure 2.3: Simulation results of BER performance when EGC is used in receiver diversity (CM1)
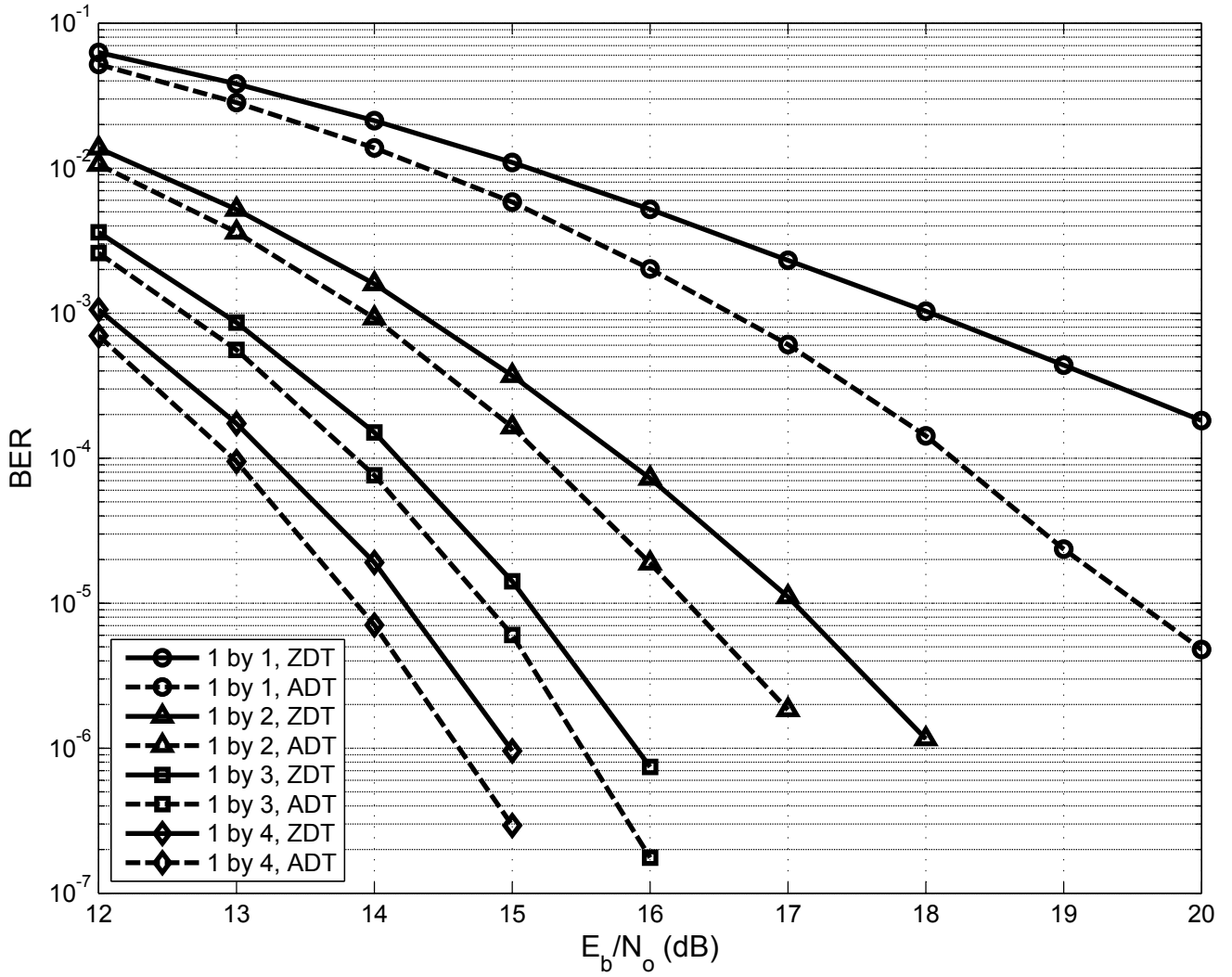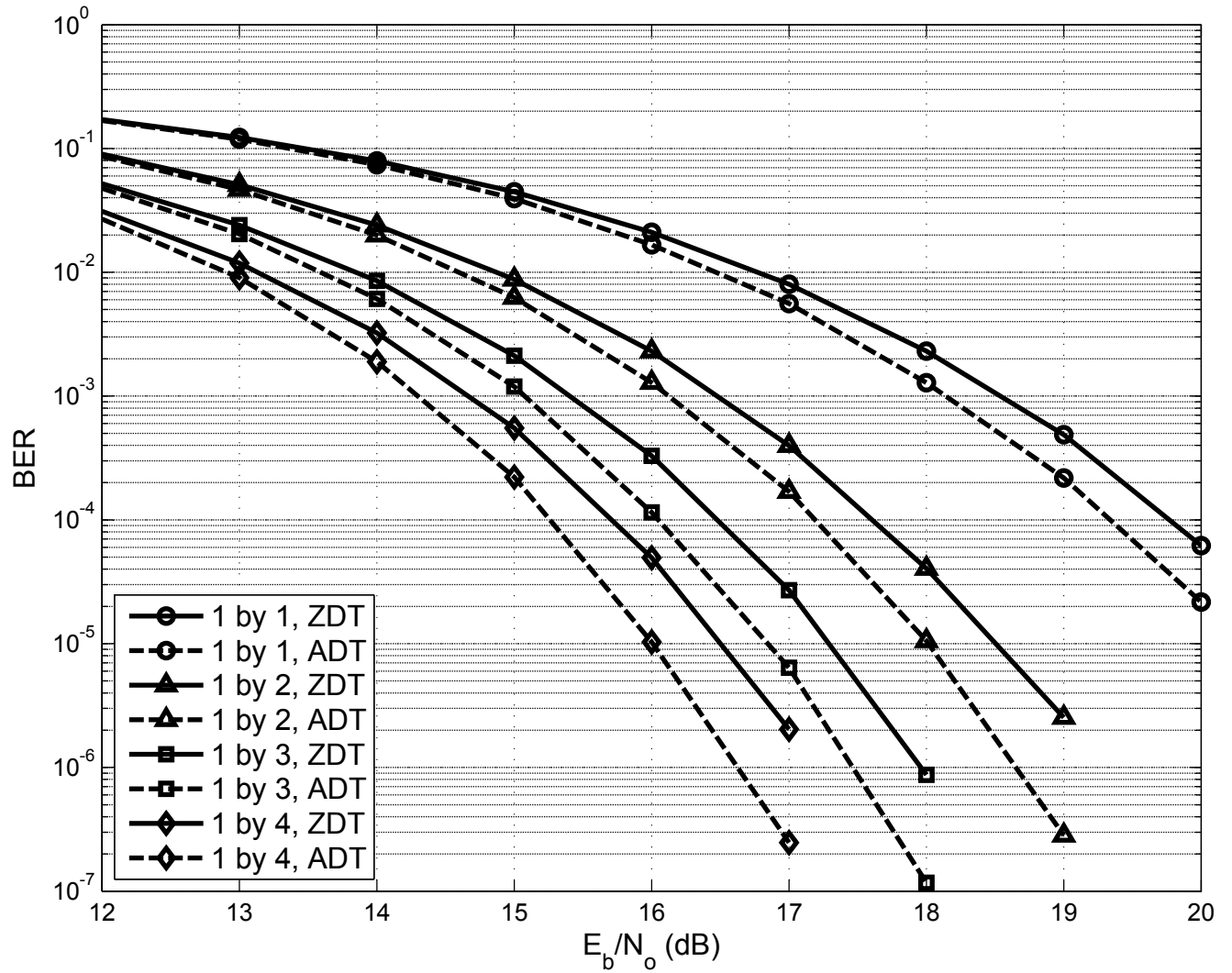
Figure 2.4: Simulation results of BER performance when EGC is used in receiver diversity (CM8)
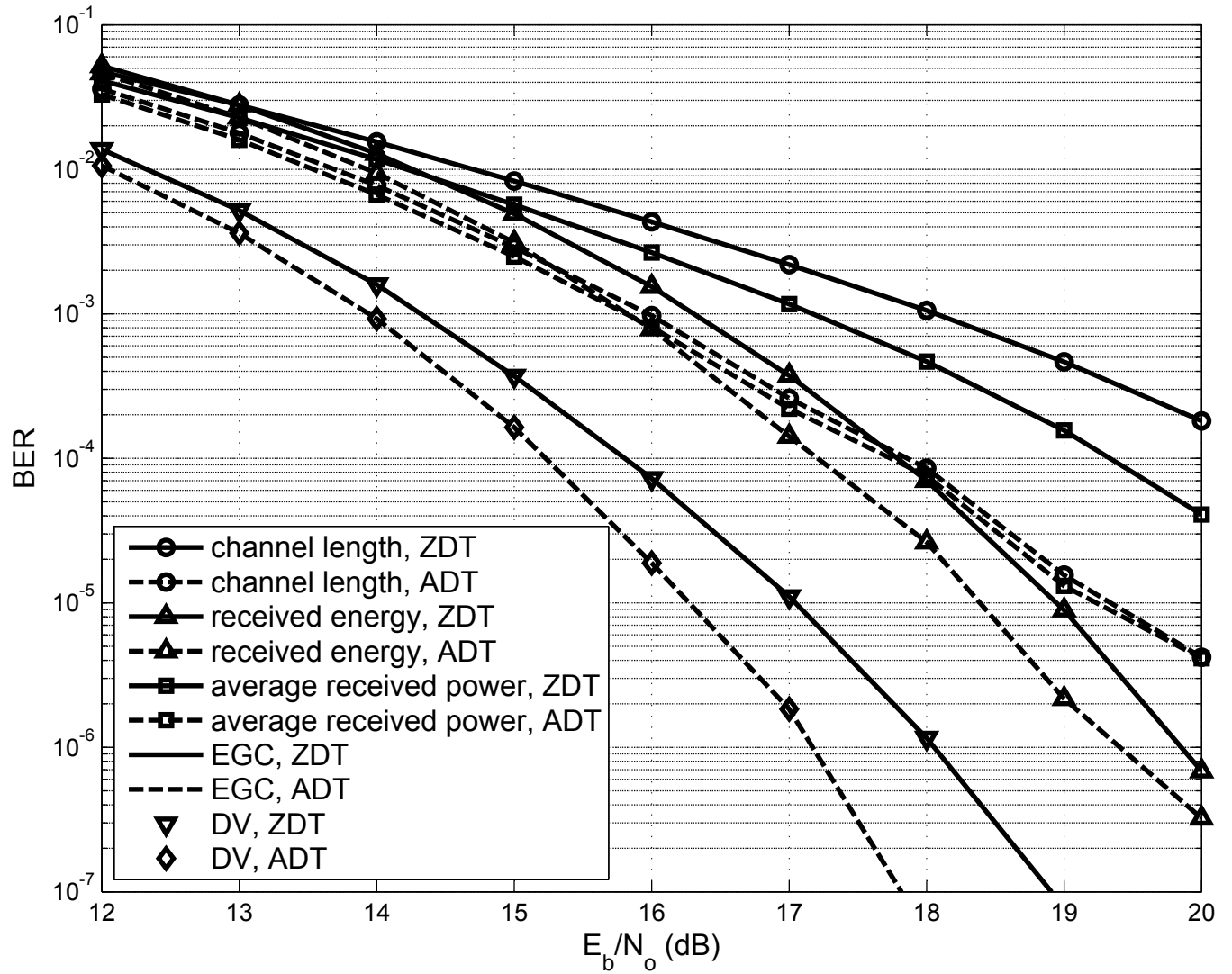
Figure 2.5: Simulation results of BER performance utilizing different receiver antenna selection criteria with 2 receiver antennas in CM1 channels
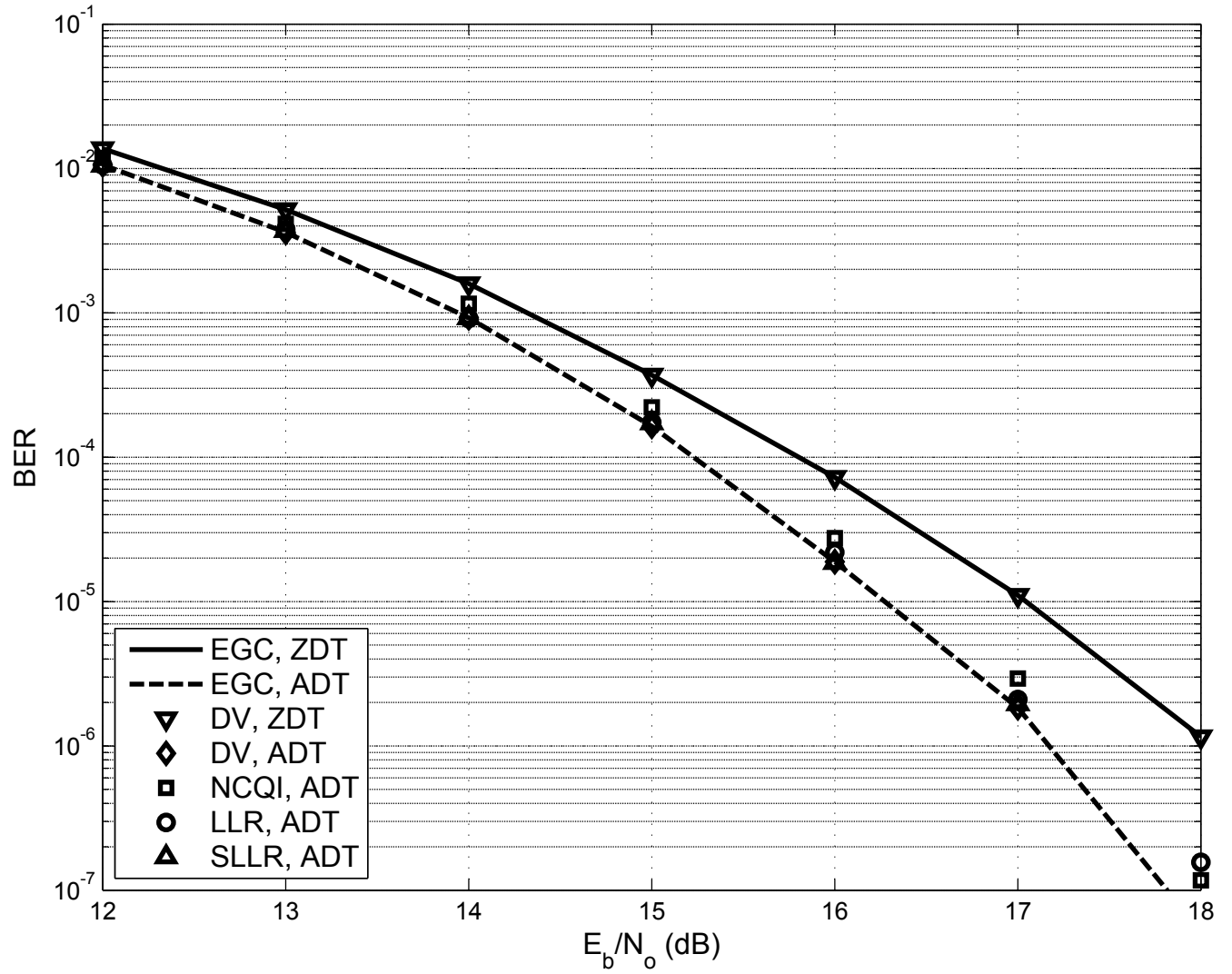
Figure 2.6: Simulation results of BER performance utilizing different receiver antenna selection criteria with 2 receiver antennas in CM1 channels

Figure 2.7: Comparison between numerical and simulation results with EGC and antenna selection criteria in CM1 channels
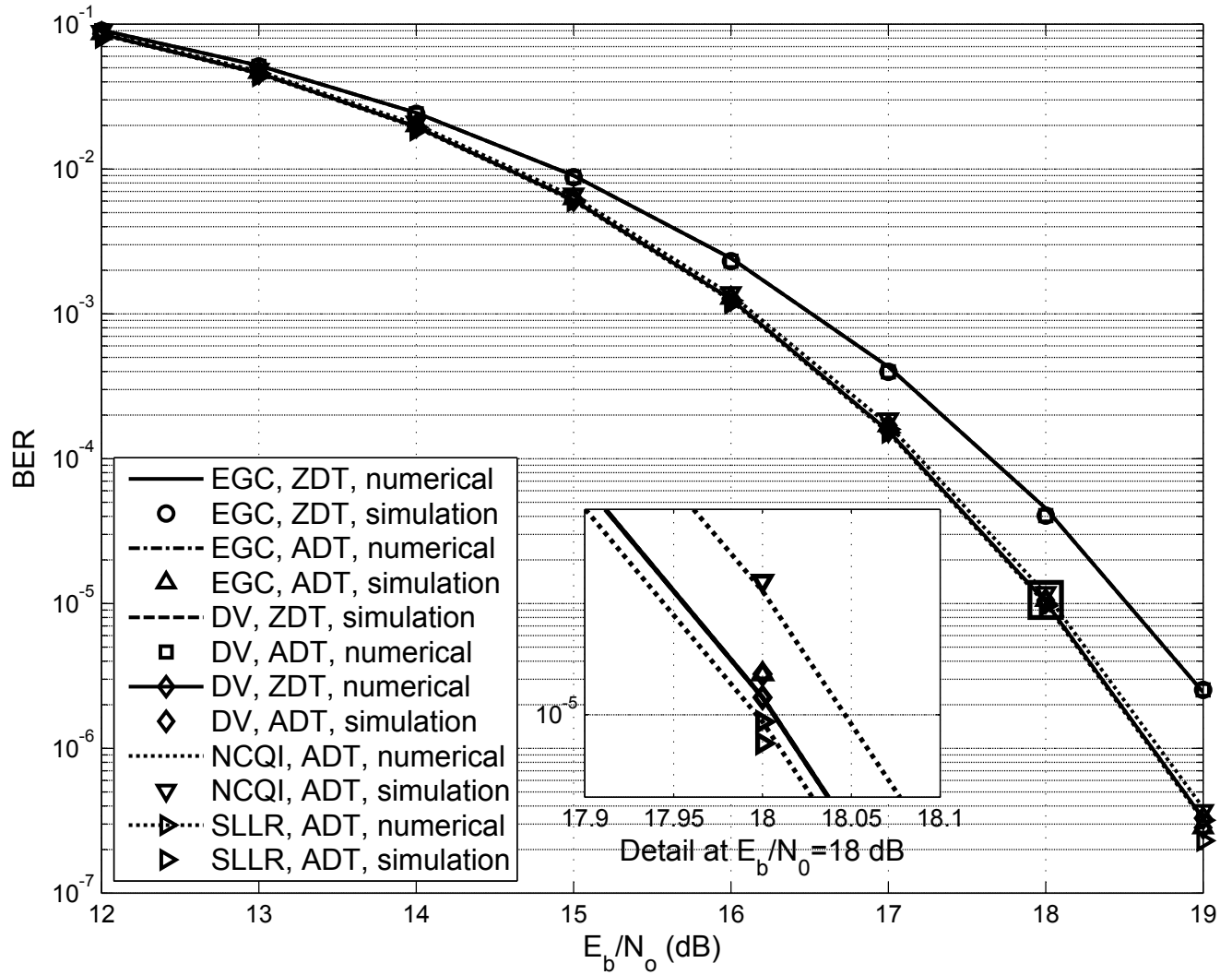
Figure 2.8: Comparison between numerical and simulation results with EGC and antenna selection criteria in CM8 channels
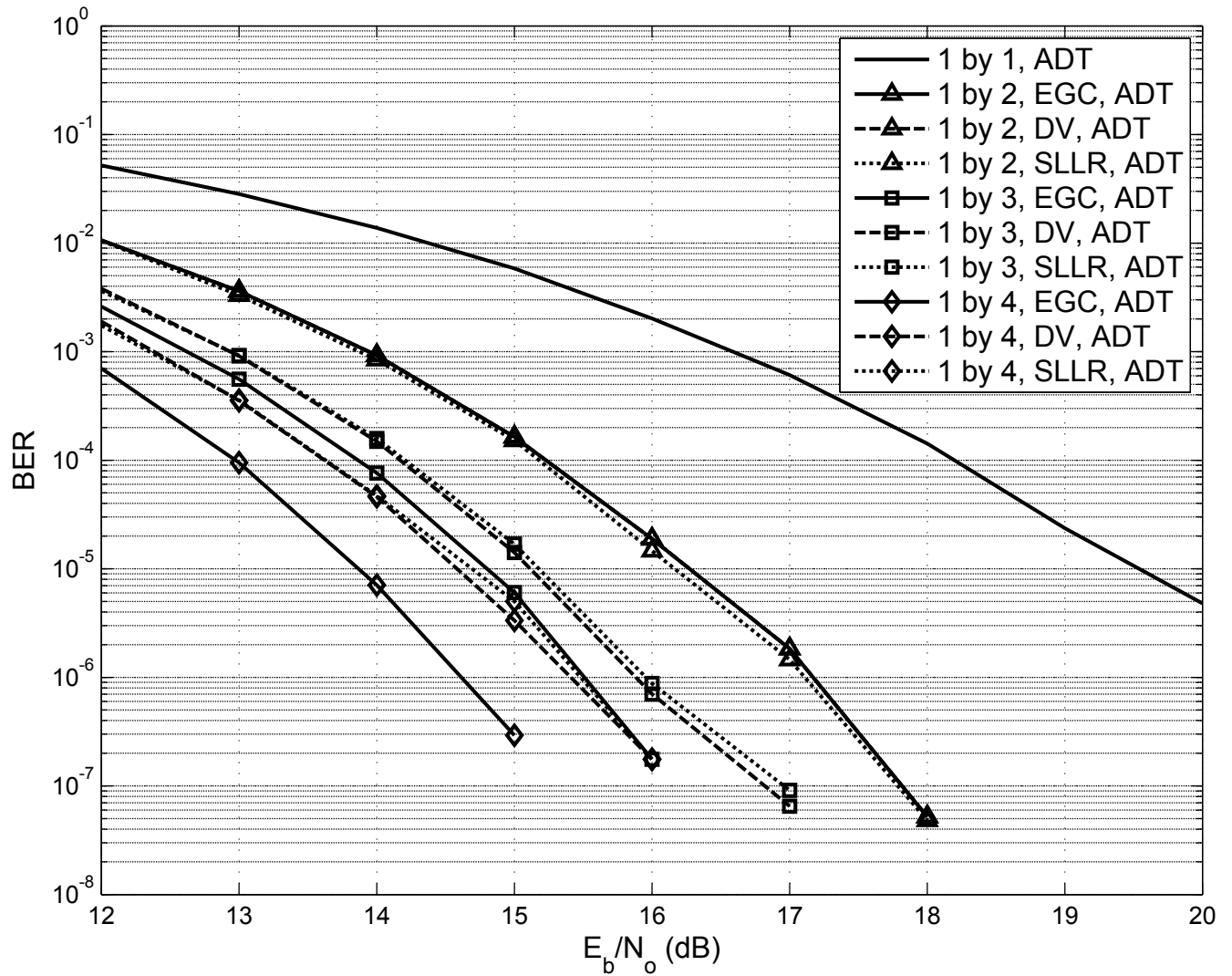
Figure 2.9: BER performance of different diversity schemes with more than 2 receiver antennas in CM1 channels (simulation results)
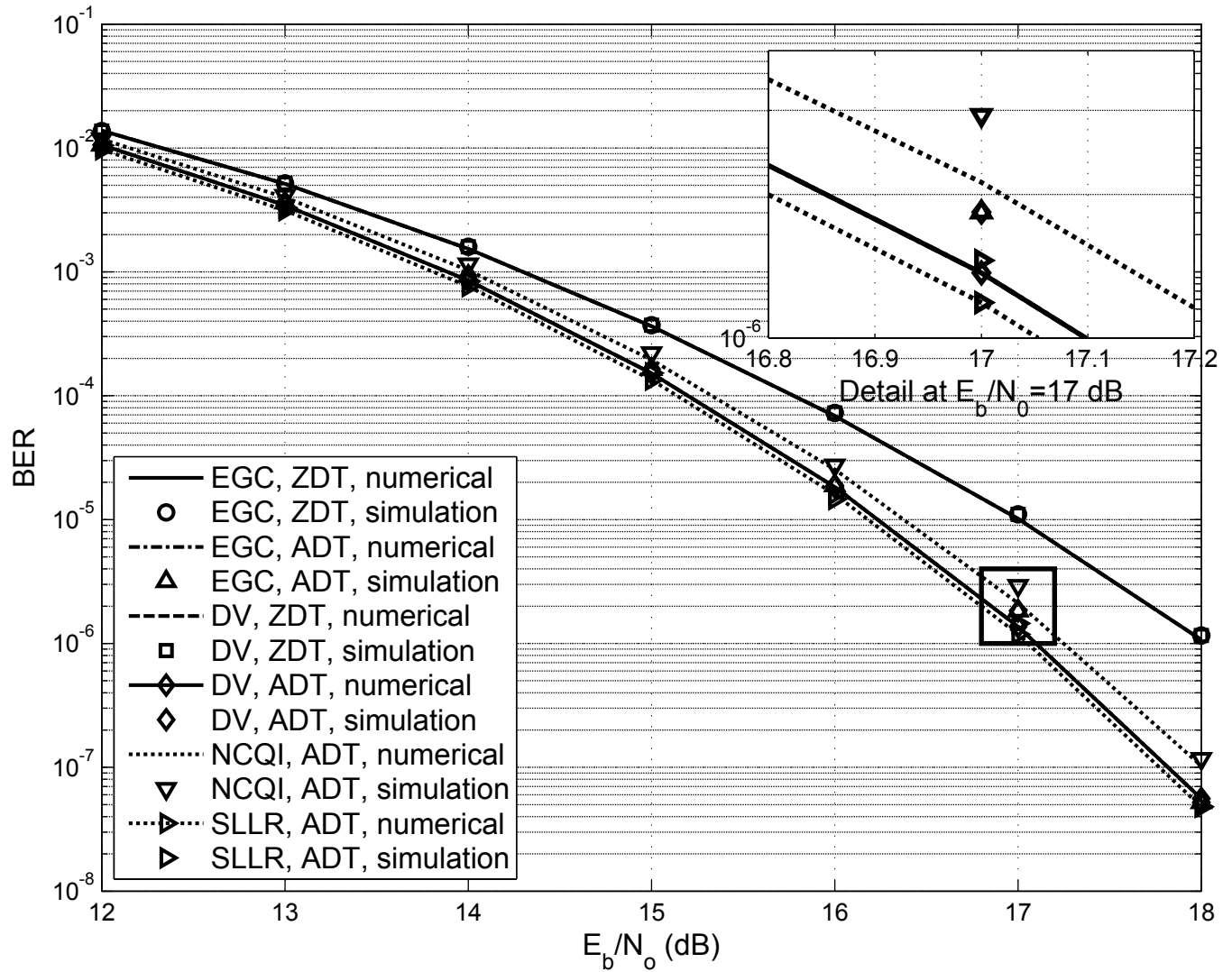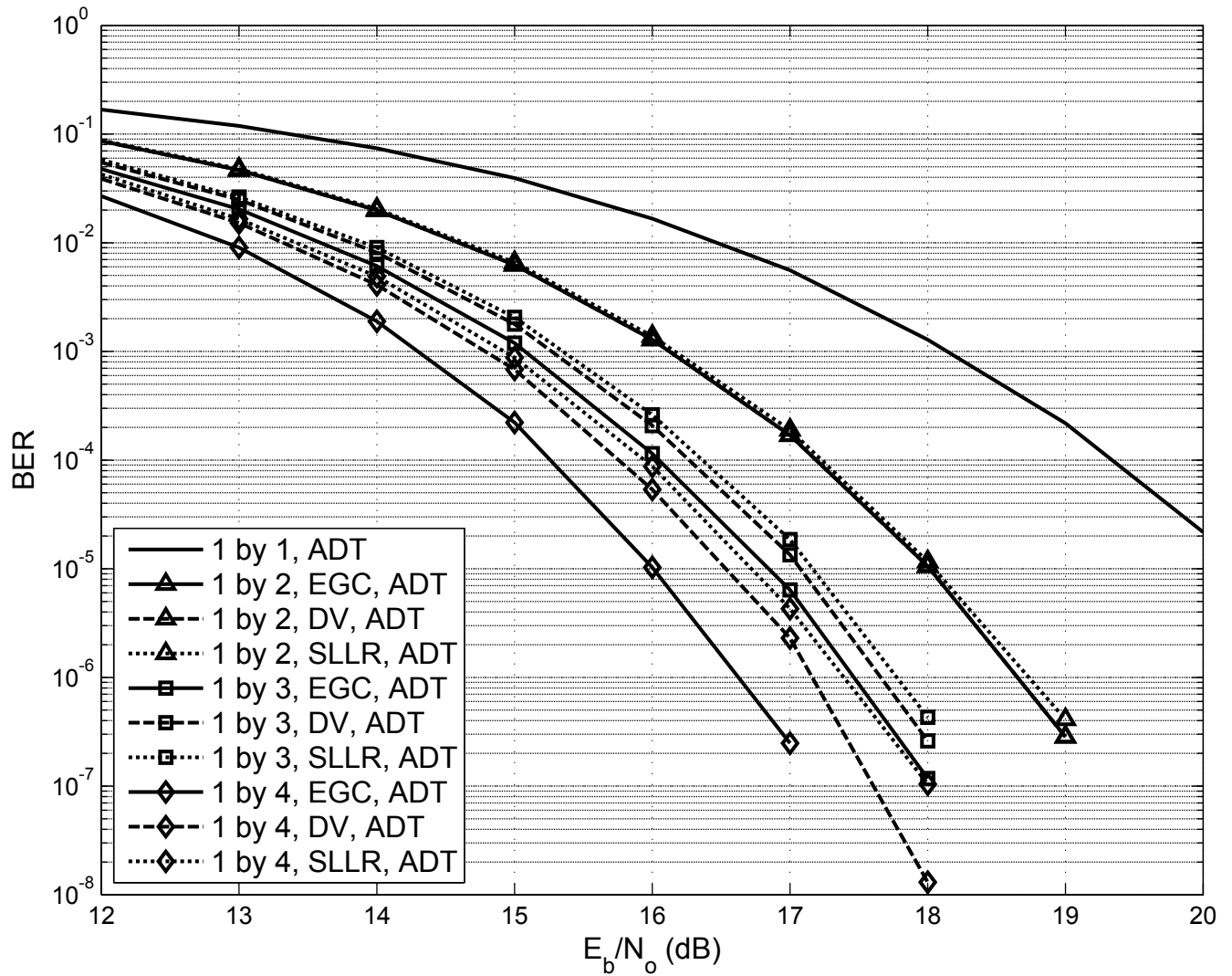
Figure 2.10: BER performance of different diversity schemes with more than 2 receiver antennas in CM8 channels (simulation results)

Chapter 3

Transmitter Diversity

3.1 System Model

In Chapter 2, different receiver diversity schemes for TRPC have been studied and compared. Different copies of the transmitted signal are received at each receiver antenna to achieve receiver antenna diversity. In a similar way, we can implement transmitter antenna diversity by sending the same signal at different transmitter antennas which will increase the number of received copies as well.

3.1.1 Delay Diversity

Delay diversity is one way to realize transmitter diversity in a multiple antenna transmitter. The same data symbol will be sent from each transmitter antenna in turn. We denote the TRPC signal as $s(t)$, so the received signal $r(t)$ will be

$$r(t) = \sum_n s[t - (n-1)T] * h_n(t) \tag{3.1}$$

Here T means the time interval between different transmitted symbols, which will be long enough to avoid inter-symbol interference. $h_n(t)$ is the n-th channel realization. At the receiver side, the received signal will be divided into multiple time slots. After that, the receiver will perform combining or selection as we discussed in Section 2.1.

This method of delay diversity will have a diversity gain at the price of lower data rate. If we implement M antennas at the transmitter, the data rate will be $1/M$ of the single antenna case. Otherwise, if the data rate remains the same, then the transmitting power should be much larger. This is not practical in most cases due to the strict power spectral density (PSD) constraint by FCC.

3.1.2 Direct Sum

The direct sum method requires all the transmitter antennas to send the data symbol at the same time. The received signal is given by

$$r(t) = \sum_i s(t) * h_i(t) \tag{3.2}$$

In this case, the data rate is increased compared with delay diversity. However, it will be impossible to separate the signals coming from different transmit antennas at the receiver end. So we can not perform any combining or selection of the transmitted antenna signal at the receiver side.

3.1.3   Transmitter Antenna Selection

In transmitter antenna selection, the transmitters send a training sequence through every antenna in turn. Then the receiver helps to select one of the transmitter antennas based on certain selection criteria and then the selected transmitter antenna index is fed back to the transmitter to be used for the subsequent data transmission. The selection criteria we propose are similar to the criteria in the receiver antenna selection section. The difference is, the transmit antenna selected through training sequence is used for the whole data sequence transmission until another training sequence is sent to update antenna selection. However, receiver antenna selection is done for every single symbol. We send a training sequence consisting of N_t symbols from each transmitter in turn, and then calculate certain selection criteria at the receiver to determine which transmit antenna should be selected. In our simulation, the length of the training sequence N_t is 64.

1. transmitter antenna selection based on averaged NCQI

   Equation (2.15) gives the definition of NCQI for a single symbol. Here we need the mean of NCQI in the whole training sequence, which is

   $$E(NCQI)_i = \frac{1}{N_t} \sum_{n=1}^{N_t} \frac{\left| D_{i,n} - \hat{\xi}_i \right|}{E_i} \tag{3.3}$$

   where i is the index representing the ith transmitter antenna and n is the index for decision variables in the training sequence. So all the transmitter antennas send a training sequence in turn and the receiver calculates $E(NCQI)_i$ for each transmit antenna. And the index of the selected transmit antenna will be

$i_{NCQI} = \arg\max_i (E(NCQI)_i)$. This will be the only antenna that transmits data to the receiver in the next data phase.

2. transmitter antenna selection based on averaged LLR

Similarly, we can also use the mean of the LLR as the selection criteria.

$$E(LLR)_i = \frac{1}{N_t} \sum_{n=1}^{N_t} \log\left[\frac{\sigma_i\left(-\hat{b}_n\right)}{\sigma_i\left(\hat{b}_n\right)}\right] + \frac{\left[D_{i,n} - m_i\left(-\hat{b}_n\right)\right]^2}{2\sigma_i^2\left(-\hat{b}_n\right)} - \frac{\left[D_{i,n} - m_i\left(\hat{b}_n\right)\right]^2}{2\sigma_i^2\left(\hat{b}_n\right)}$$

(3.4)

where $\hat{b}_n$ is the expected bit for the nth symbol in the training sequence. In our simulation, $\hat{b}_n$ is given as

$$\hat{b}_n = \begin{cases} +1, & \text{n is odd} \\ -1, & \text{n is even} \end{cases}$$

(3.5)

The index of the selected transmit antenna will be $i_{LLR} = \arg\max_i (E(LLR)_i)$.

3. transmitter antenna selection based on averaged SLLR

The averaged LLR is very complicated to implement. Simplify it and we get averaged SLLR

$$E(SLLR)_i = \sum_{n=1}^{N_t} \frac{2E_i\left|D_{i,n} - \hat{\xi}_i\right|}{\sigma_i^2 N_t}$$

(3.6)

4. transmitter antenna selection based on SCQI

Since we only need the mean for the training sequence, which has half +1

symbols and half -1 symbols. Based on these features we can further simplify the averaged SLLR as follows.

From (2.19), we have the definition of SLLR

$$
\begin{aligned}
SLLR_{i,n} &= \frac{\left| D_{i,n} - \hat{\xi}_i \right|}{\sigma_i^2} \\
&= \begin{cases}
\frac{2E_i \left(D_{i,n} - \hat{\xi}_i \right)}{\sigma_i^2}, & \hat{b}_n = +1 \\[2mm]
\frac{-2E_i \left(D_{i,n} - \hat{\xi}_i \right)}{\sigma_i^2}, & \hat{b}_n = -1
\end{cases}
\end{aligned}
\tag{3.7}
$$

So we can get the approximated mean of SLLR as

$$
\begin{aligned}
E(SLLR)_i &= \frac{\sum_{\hat{b}_n=+1} SLLR_{i,n} + \sum_{\hat{b}_n=-1} SLLR_{i,n}}{N_t} \\
&= \frac{2E_i \left(\sum_{\hat{b}_n=+1} D_{i,n} - \sum_{\hat{b}_n=+1} \hat{\xi}_i \right) - 2E_i \left(\sum_{\hat{b}_n=-1} D_{i,n} - \sum_{\hat{b}_n=-1} \hat{\xi}_i \right)}{\sigma_i^2 N_t} \\
&\approx \frac{2E_i \left[\frac{N_t}{2} m(+1) - \frac{N_t}{2} m(-1) - \frac{N_t}{2} \hat{\xi}_i + \frac{N_t}{2} \hat{\xi}_i \right]}{\sigma_i^2 N_t} \\
&= \frac{E_i \left[m(+1) - m(-1) \right]}{\sigma_i^2} \\
&= \frac{2E_i^2}{\sigma_i^2}
\end{aligned}
$$

$$\tag{3.8}$$

where $m(+1)$ is the mean for all the $+1$ symbols. And E_i is defined as $(m(+1) - m(-1))/2$. We approximate the sum of all the symbols that are decoded as $+1$ to be $\frac{N_t}{2} m(+1)$. The precision of this approximation depends on the bit error

rate. Because there are N_t symbols in the transmitted signal. If the bit error rate is relatively low, there will be almost $N_t/2$ symbols recognised as +1 at the receiver side. The same thing also applies to -1 symbols. Therefore this approximation can further reduce the complexity of the selection criteria for transmitter diversity in high SNRs. We name $\frac{2E^2}{\sigma^2}$ as Simplified Channel Quality Indicator (SCQI) for convenience.

3.2 Numerical Analysis on Transmitter Diversity

In our numerical analysis, we consider a system with 2 transmitter antennas and 1 receiver antenna in accordance with the simulation.

3.2.1 Delay Diversity with Combining and Selection

The transmitter antennas send the information data in turn. The delay between different antennas is set to be long enough to avoid inter-symbol interference (ISI). Here, we only consider 2 transmitter antennas. So if we want to keep the same BER, the total transmitting power will be doubled compared with 1-by-2 receiver diversity scheme. This means delay diversity requires 3 dB higher SNR to achieve the same BER performance of receiver diversity. In Section 2.2, we investigated receiver diversity with EGC, selection based on DV, NCQI and SLLR. The numerical analysis of delay diversity is the same as receiver diversity. The only difference between them is the SNR. If we shift the results of BER performance of receiver diversity by 3 dB, we can obtain the results for delay diversity.

3.2.2 Antenna Selection

The transmitter antenna selection schemes are described in Section 3.1. In our numerical analysis, four antenna selection criteria are considered, which are averaged NCQI, averaged LLR, averaged SLLR and SCQI.

The averaged NCQI of the ith transmitter antenna can be calculated as

$$
\begin{aligned}
E(NCQI)_i &= \int f(D)\frac{|D-\xi_i|}{E_i}\mathrm{d}D \\
&= \frac{1}{2}\int_{-\infty}^{\infty}\frac{1}{\sqrt{2\pi\sigma_i^2(+1)}}\exp\left(\frac{-(x-\mu_i^2(+1))^2}{2\sigma_i^2(+1)}\right)\frac{|x-\xi_i|}{E_i}\mathrm{d}x \\
&\quad + \frac{1}{2}\int_{-\infty}^{\infty}\frac{1}{\sqrt{2\pi\sigma_i^2(-1)}}\exp\left(\frac{-(x-\mu_i(-1))^2}{2\sigma_i^2(-1)}\right)\frac{|x-\xi_i|}{E_i}\mathrm{d}x
\end{aligned}
\tag{3.9}
$$

where μ_i and σ_i^2 are the mean and variance of D_i respectively. $\xi = \frac{1}{2}(m(+1)+m(-1))$ is the ADT and $E = \frac{1}{2}(m(+1)-m(-1))$. Using the results in Section 2.2, we can approximate DV as a Gaussian RV and get μ and σ by numerical calculation. Then we have $i_{NCQI} = \arg\max_i (E(NCQI)_i)$.

Similarly, the averaged LLR, averaged SLLR and SCQI can be calculated respectively by

$$
E(LLR)_i = \int f(D)\left(\log\left[\frac{\sigma_i\left(-\hat{b}\right)}{\sigma_i\left(\hat{b}\right)}\right] + \frac{\left[D-m\left(-\hat{b}\right)\right]^2}{2\sigma_i^2\left(-\hat{b}\right)} - \frac{\left[D-m\left(\hat{b}\right)\right]^2}{2\sigma_i^2\left(\hat{b}\right)}\right)\mathrm{d}D
\tag{3.10}
$$

$$
E(SLLR)_i = \int f(D)\frac{2E_i\left|D-\hat{\xi}_i\right|}{\sigma_i^2}\mathrm{d}D
\tag{3.11}
$$

$$E(SCQI)_i = \frac{2E_i^2}{\sigma_i^2} \tag{3.12}$$

Once we get the selection criteria for each training sequence, we can determine the index of the selected antenna. The final BER is the BER of this selected antenna, which can be calculated as $Pe|_{ZDT} = \frac{1}{2}Q\left(\frac{-m(-1)}{\sqrt{\sigma^2(-1)}}\right) + \frac{1}{2}Q\left(\frac{m(+1)}{\sqrt{\sigma^2(+1)}}\right)$ and $Pe|_{ADT} = \frac{1}{2}Q\left(\frac{-(m(-1)-\xi)}{\sqrt{\sigma^2(-1)}}\right) + \frac{1}{2}Q\left(\frac{m(+1)-\xi}{\sqrt{\sigma^2(+1)}}\right)$.

3.3 Simulation and Numerical Results for Transmitter Diversity

In this section, we present the simulation and numerical results for transmitter diversity in TRPC systems. The channel model used in the numerical calculation and simulation are 802.15.4a CM1 and CM8 [11]. CM1 is a representative for the line-of-sight (LOS) channels which has relatively short channel length and less multipath components. On the contrary, CM8 represented the non-line-of-sight (NLOS) channels which have the longest channel length and many more multipath components. These two typical channel models can cover the most common channels in practise. The system setup is the same as in Section 2.3. We generated 100 realizations of 802.15.4a channels for every transmitter antenna and get the average of their BERs as the result.

From Fig. 3.1, we can see that direct sum has the worst performance among all the transmitter diversity methods. There are many multipath components in the channel impulse response which will cover a much longer time period than the

pulse cluster duration. In this case, there will be lots of overlaps in the sum of 2 different transmitted signals. In addition, the received signal contains noise from both transmitter antennas and it is impossible to separate them at the receiver side. All these factors contribute to the poor performance of the direct sum scheme. In addition, transmitter antenna selection schemes outperform delay diversity by a large performance gap. Among all the selection criteria, averaged NCQI shows as the worst case while averaged SLLR and SCQI have the best BER performance.

Fig. 3.2 and Fig. 3.3 illustrate that the numerical analysis agrees with the simulation well. There is a small gap between numerical and simulation results, which is probably due to the approximation in numerical analysis where we formulate the decision variable as Gaussian distributed. Both simulation and numerical analysis show that averaged SLLR and SCQI have the same BER performance and are the best among all these selection criteria. SCQI should be our choice for transmitter antenna selection criteria because of its lower implementation complexity over averaged SLLR.

Fig. 3.4 shows the simulation results of 2-by-1 and 4-by-1 transmitter delay diversity in CM1 channels. In order to utilize delay diversity, the transmitter antennas send the same data symbols in turn. The receiver antenna will get N copies of data symbols if there were N transmitter antennas. Based on these N copies of data symbols, the receiver will perform equal gain combining or selection. The delay diversity for transmitter antennas will be similar to receiver diversity. They all have multiple copies of the data symbols at the receiver side. And combining or selection will be implemented at the receiver. The only difference between these two schemes is that, the data rate for transmitter diversity will be lower since it uses several transmitter

antennas to send the same data in turn. Therefore, if we have two systems, system 1 has N transmitter antennas and 1 receiver antenna. System 2 has 1 transmitter antenna and N receiver antennas. System 1 utilizes transmitter delay diversity with combining and system 2 utilizes receiver diversity with combining. If all the other conditions are the same, the BER performance of system 1 is expected to be $10 \log_{10} N$ dB worse than system 2. Here if $N = 2$, transmitter delay diversity will be 3 dB worse than that of receiver diversity. This agrees with the simulation results in section 2.3. Because of this 3 dB degradation, the BER performance of transmitter delay diversity in Fig. 3.4 is even worse than 1-by-1 system. So transmitter delay diversity will be much worse than antenna selection.

Fig. 3.5 shows the BER performance of transmitter antenna selection based on SCQI in both CM1 and CM8 channels. We can see that each additional transmitter antenna with selection based on SCQI has a performance gain of 0.8 dB, 0.2 dB and 0.1 dB at BER $= 10^{-3}$ in CM1 channels. And in CM8 channels, the gains are 0.4 dB, 0.05 dB and 0.03 dB. The overall performance gain was not as good as that of receiver diversity shown in Section 2.3. That is because only one transmitter antenna is chosen for the transmission of the whole packet in transmitter antenna selection. The selection is essentially based on the multipath channel realizations corresponding to different transmit antennas. While in receiver diversity, we can select each symbol from different receiver antennas and the selection is essentially based on not only the multipath channel realizations corresponding to receive antennas but also the instantaneous noise realizations at each symbol. Therefore, a transmitter design with 2 antennas is a good balance between performance and cost.

Fig. 3.6 compares the BER performance of 1-by-1, 1-by-2, 2-by-1 and 2-by-2

systems in CM1 channels. We can see that when the receiver utilizes EGC with ZDT, 2-by-2 system utilizing transmitter antenna selection based on SCQI shows 0.6 dB gain at BER $= 10^{-5}$ over 1-by-2 system. A similar gain is achieved when the receiver utilizes selection based on SLLR. In our simulations, all the combinations of receiver and transmitter diversity schemes have been tried and the best case is that transmitter selection based on SCQI and receiver selection based on SLLR. For 1-by-1 ADT system, it achieves BER $= 10^{-5}$ at 19.5 dB. So 2-by-2 system with SCQI & SLLR outperforms that by 3.8 dB. We can also see that 2-by-1 system performs much worse than 1-by-2 system, which means receiver diversity is more effective than transmitter diversity here. Fig. 3.6 also compares the numerical analysis with simulation results for 2-by-2 system. The gaps between them are still acceptable. Fig. 3.7 represents the BER performance of 2-by-2 system in CM8 channels. The performance improvement of 2-by-2 system with SCQI & SLLR is 2.6 dB over 1-by-1 at BER $= 10^{-5}$ in CM8 channels.

3.4   Summary

In this chapter, we have discussed several multi-antenna transmitter diversity schemes, including direct sum, delay diversity and selection diversity. Among them, selection diversity shows the best BER performance. But the performance gain is not as significant as in receiver diversity schemes, especially with more than 2 transmitter antennas. In addition, we have proposed SCQI, which is proved to be the best selection criteria for transmitter antenna selection. Meanwhile, SCQI is also the easiest selection criteria for implementation. Therefore, for a 2-by-2 system, it achieves the

best BER performance when transmitter antenna selection is based on SCQI and receiver antenna selection is based on SLLR.
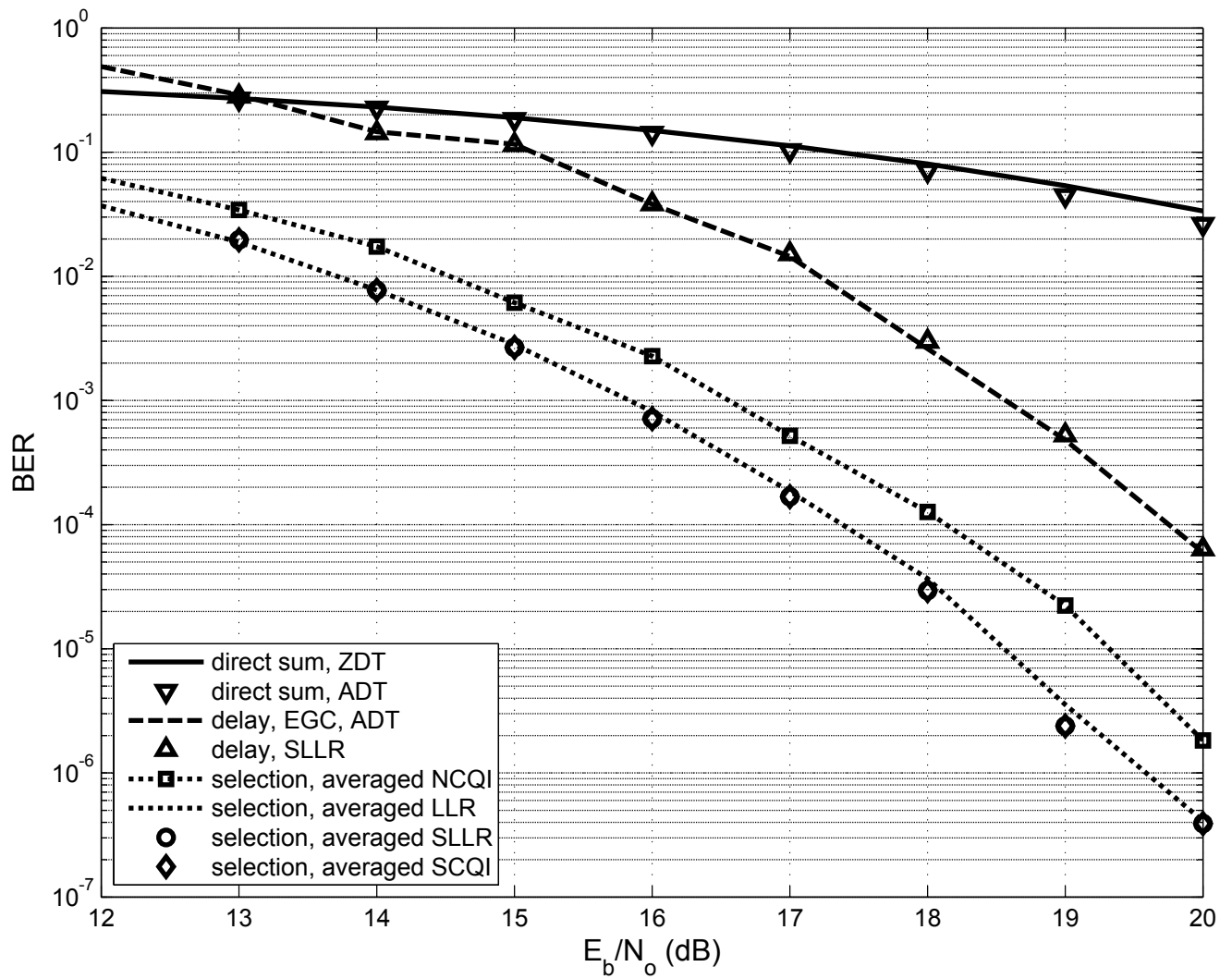
Figure 3.1: The BER performance of transmitter diversity (2-by-1) in CM1 channels
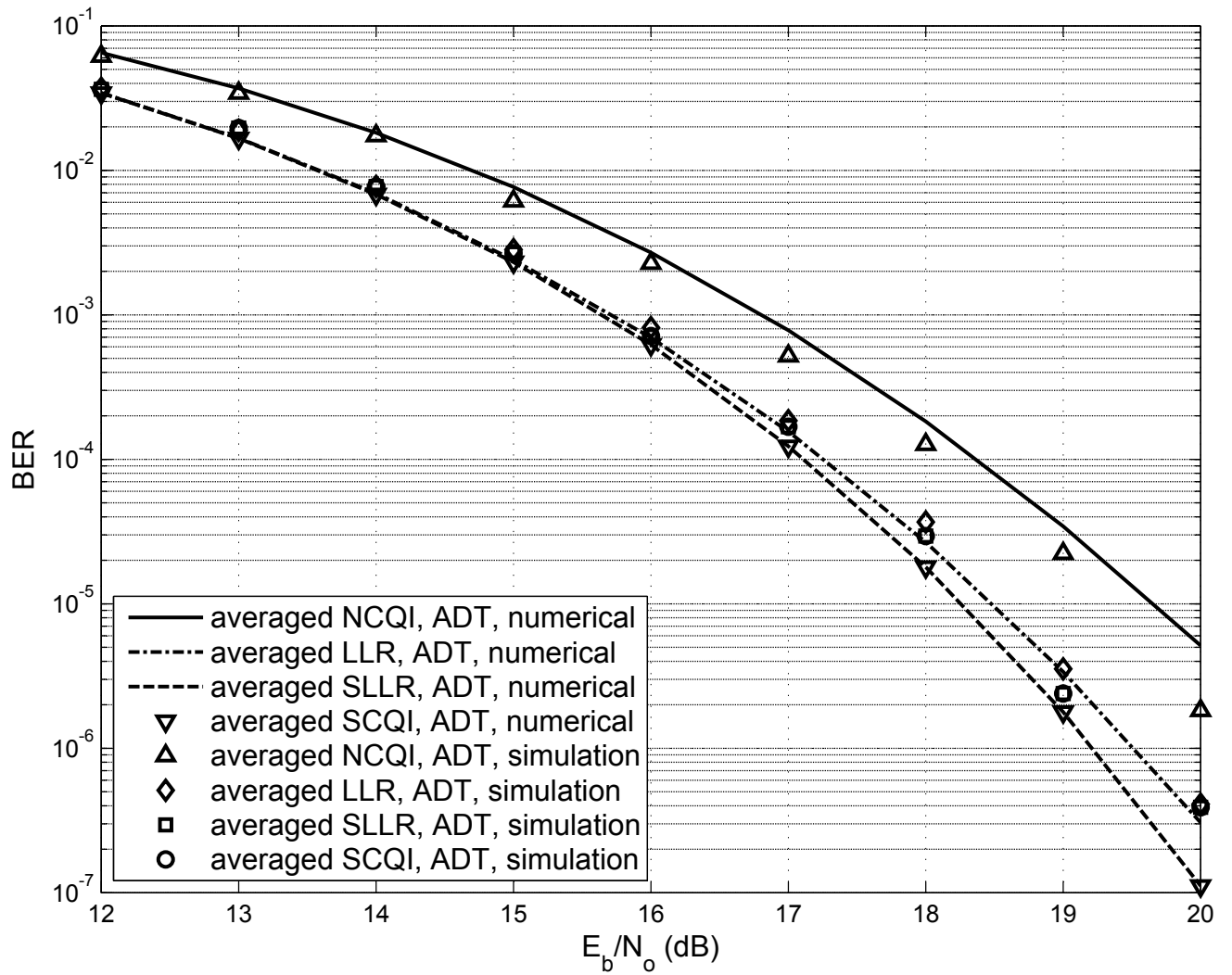
Figure 3.2: The BER performance of simulation and numerical analysis for transmitter diversity (2-by-1) with antenna selection in CM1 channels
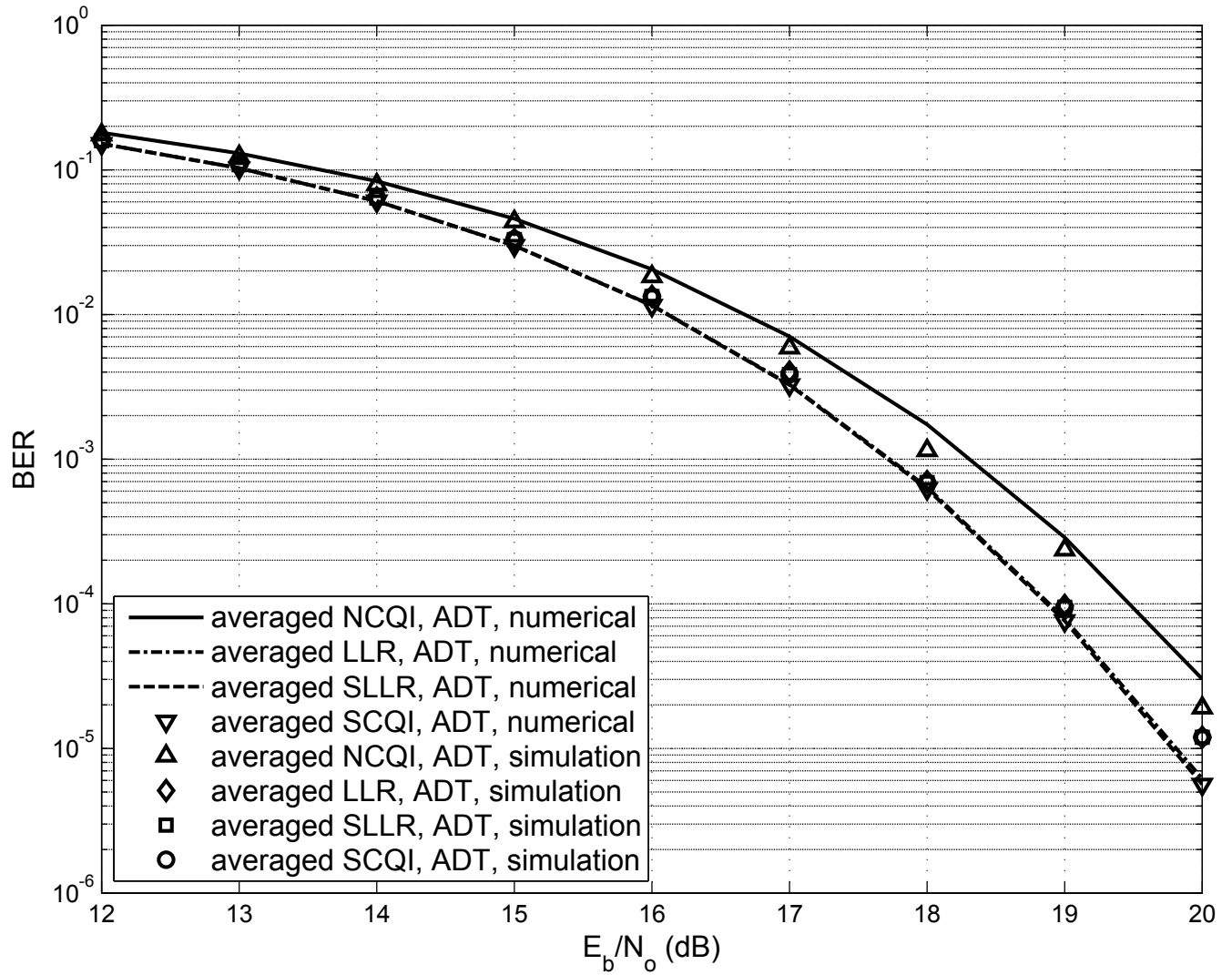
Figure 3.3: The BER performance of simulation and numerical analysis for transmitter diversity (2-by-1) with antenna selection in CM8 channels
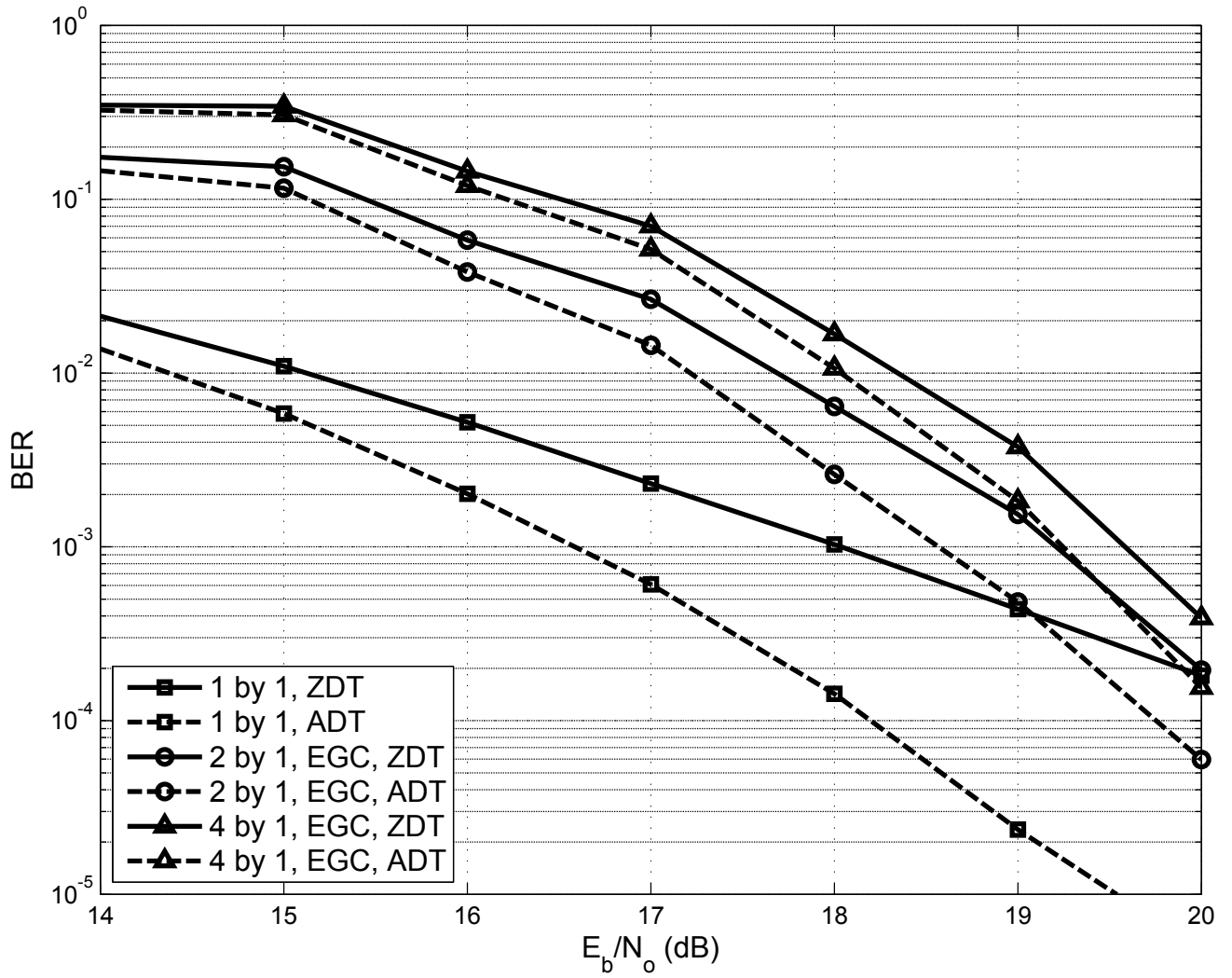
Figure 3.4: The BER performance of simulation for transmitter delay diversity in CM1 channels
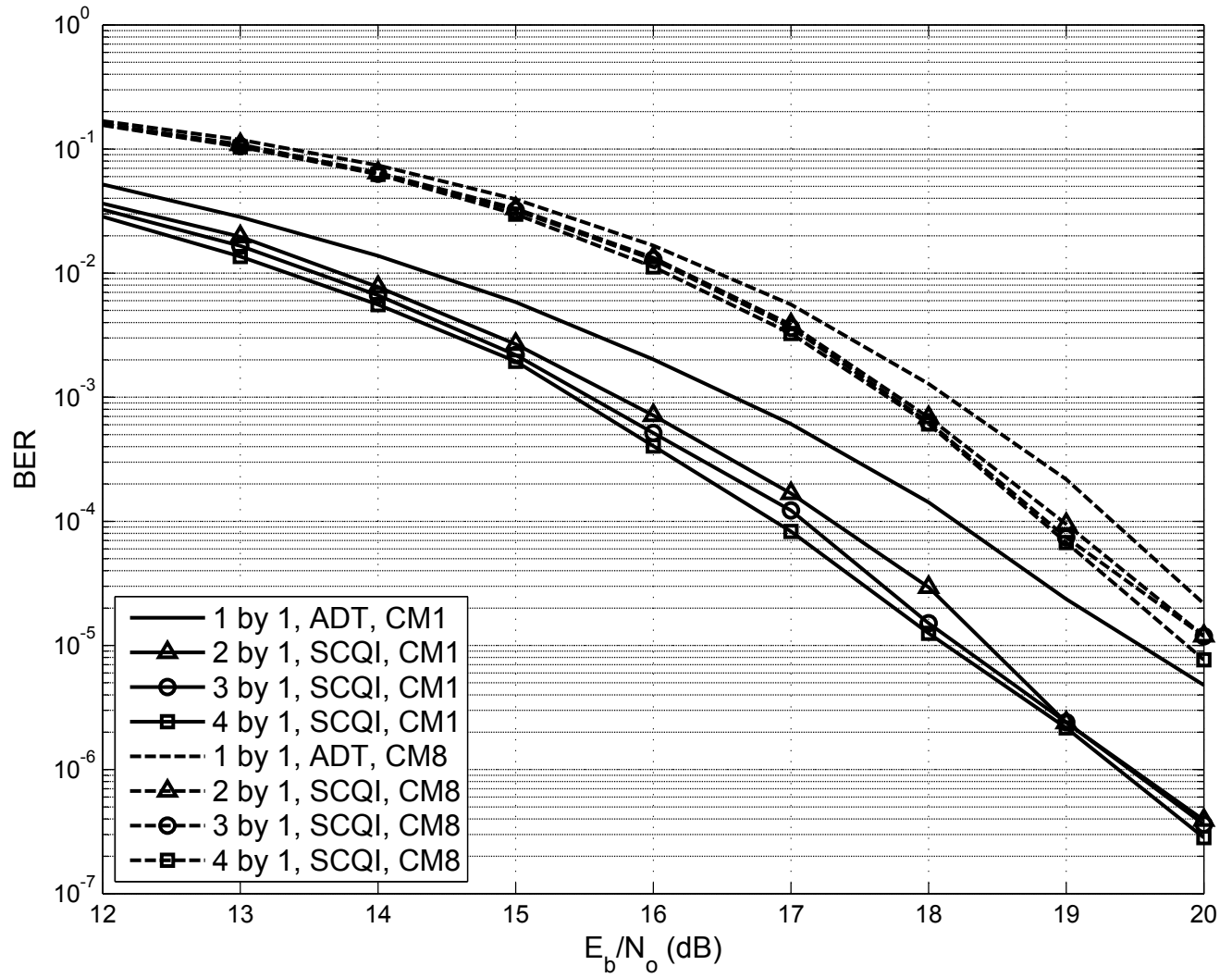
Figure 3.5: The BER performance of transmitter antenna selection based on SCQI in both CM1 and CM8 channels (simulation results)
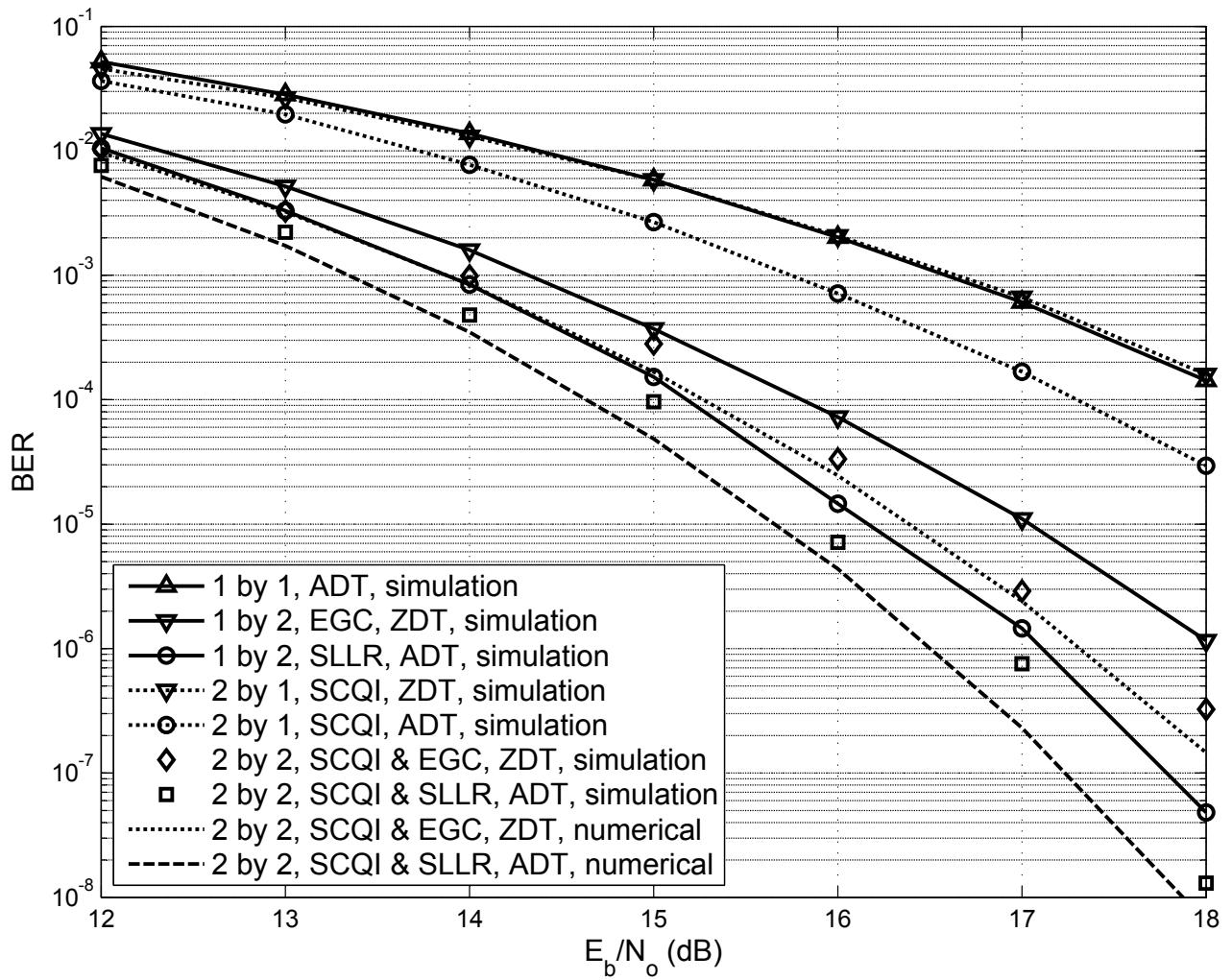
Figure 3.6: The BER performance of 2-by-2 system in CM1 channels
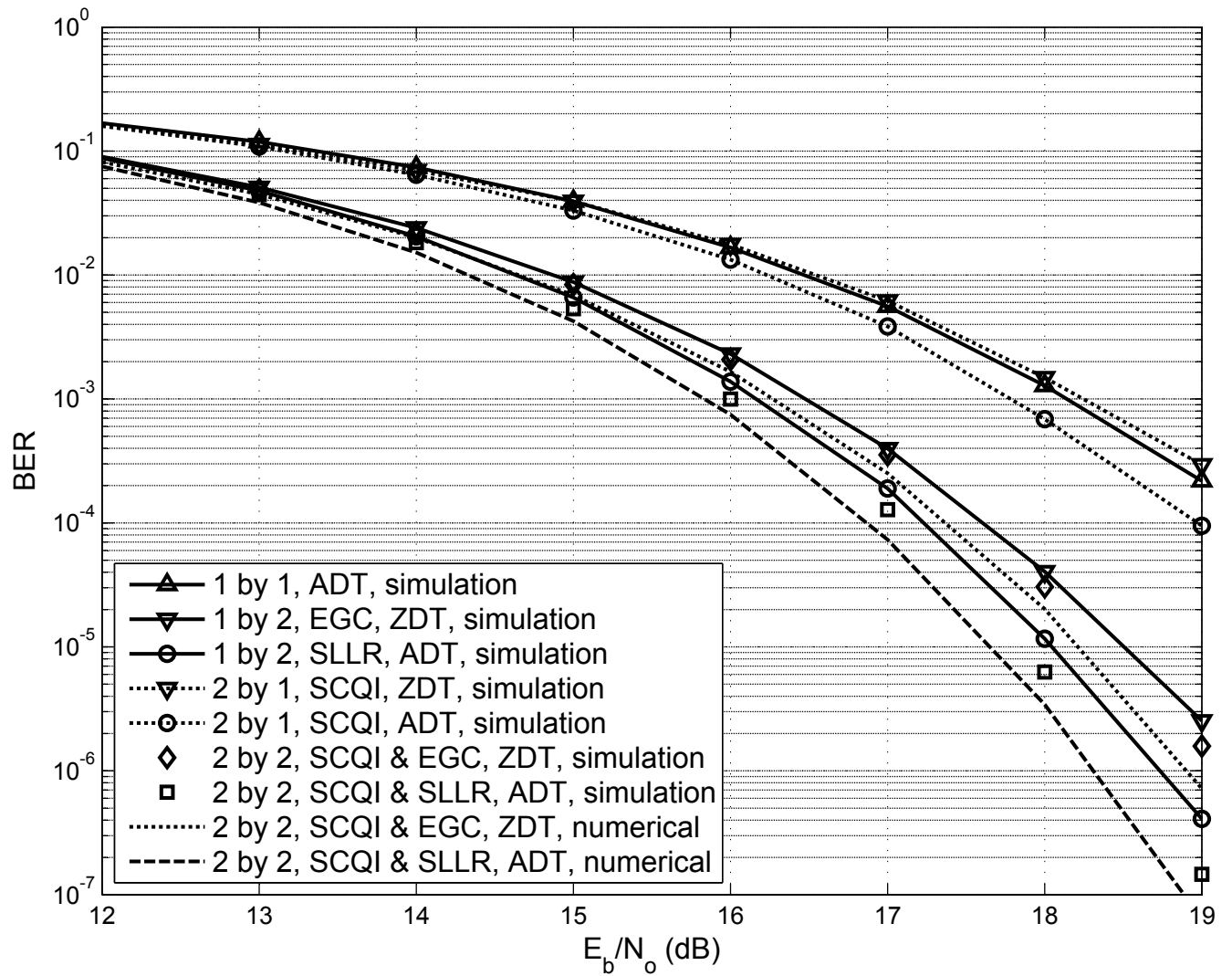
Figure 3.7: The BER performance of 2-by-2 system in CM8 channels

Chapter 4

Multiuser Downlink Schemes for TRPC

4.1 System Model

Possible applications for TRPC include sensor networks, computer peripherals and localization systems. All these scenarios require multiuser access. So it is an important research topic for UWB TRPC systems. The commonly used orthogonal spreading codes for different users will lost the orthogonality in the frequency selective multipath fading channel. To address this problem, the chip-interleaved block spreading code division multiple access (CDMA) is proposed in [18] to avoid multiuser interference (MUI). This CDMA scheme is applied to TRPC and compared with time division multiple access (TDMA) in [19]. To further improve the BER performance, we propose a new multiuser downlink scheme for TRPC in this chapter.

4.1.1 Time Division TRPC (TD-TRPC)

Time division is commonly used in multiuser downlink schemes. For example, a time division multiuser scheme for impulse radio UWB is proposed in [20]. For TRPC system, TDMA and CDMA are compared in [19]. The BER performance of them are the same but TDMA is much simpler to implement. So TDMA is the choice for multiple access in [19].

Assuming there are N users, we need to divide the symbol duration T_s into N chip intervals. So the transmitted signal can be represented as

$$s(t) = \sqrt{\frac{E_b}{2N_f}} \sum_{m=-\infty}^{\infty} \sum_{n=0}^{N-1} s_{b_{m,n}}(t - nT_c - mT_s) \tag{4.1}$$

where $b_{m,n} \in \{-1, +1\}$ is the mth bit for n^{th} user.

The received signal at the nth user is

$$r(t) = \sqrt{\frac{E_b}{2N_f}} \sum_{l=0}^{L-1} \alpha_l \sum_{m=-\infty}^{\infty} s_{b_{m,n}}(t - \tau_l - nT_c - mT_s) + n(t) \tag{4.2}$$

After the autocorrelation, we can get the decision variable D and make decisions based on ZDT or ADT. If T_s is fixed, we have $T_c = T_s/N$.

4.1.2 Pulse Pattern TRPC (PP-TRPC)

In TD-TRPC, as the number of users increases, the chip interval T_c will become shorter and shorter. When T_c is much shorter than the length of channel impulse response, there will be severe multiuser interference (MUI). To address this problem, we propose a new TRPC pulse pattern structure (PP-TRPC) to meet the needs of

a multiuser UWB system. For simplicity, we discuss a system with 2 users first. According to [16], if we denote energy per bit as E_b, number of repetition as N_f, T_s as symbol duration time, the transmitted signal of PP-TRPC can be represented by

$$s(t) = \sqrt{\frac{E_b}{2N_f}} \sum_{m=-\infty}^{\infty} s_{b_m}(t - mT_s) \tag{4.3}$$

where $b_m \in \{00, 01, 10, 11\}$. So there are four pulse patterns in PP-TRPC. Two of them are the same as original TRPC, which are s_{01} and s_{11}. In addition to that, we add two more pulse patterns in PP-TRPC, s_{00} and s_{10}. These are illustrated in Fig. 4.1 for the case of $N_f = 4$. In PP-TRPC, T_d and T_p are the same as in TRPC and $T_d = T_p$.

According to the channel model in [11], UWB channels can be denoted as

$$h(t) = \sum_{l=0}^{L-1} \alpha_l \delta(t - \tau_l) \tag{4.4}$$

where $h(t)$ is the impulse response of the channel. L, α_l and τ_l denotes the number of multipath, the amplitude and delay of the lth multipath delay respectively. So the received signal of PP-TRPC is

$$
\begin{aligned}
r(t) &= \sqrt{\frac{E_b}{2N_f}} \sum_{l=0}^{L-1} \alpha_l \sum_{m=-\infty}^{\infty} s_{b_m}(t - \tau_l - mT_s) + n(t) \\
&= \sqrt{\frac{E_b}{2N_f}} \sum_{m=-\infty}^{\infty} q_{b_m}(t - mT_s) + n(t)
\end{aligned}
\tag{4.5}
$$

where $b_m \in \{00, 01, 10, 11\}$ and $q_{b_m} = \sum_{l=0}^{L-1} \alpha_l s_{b_m}(t - \tau_l)$

If ZDT is applied, the receiver structure for user 1 and user 2 is illustrated in Fig.
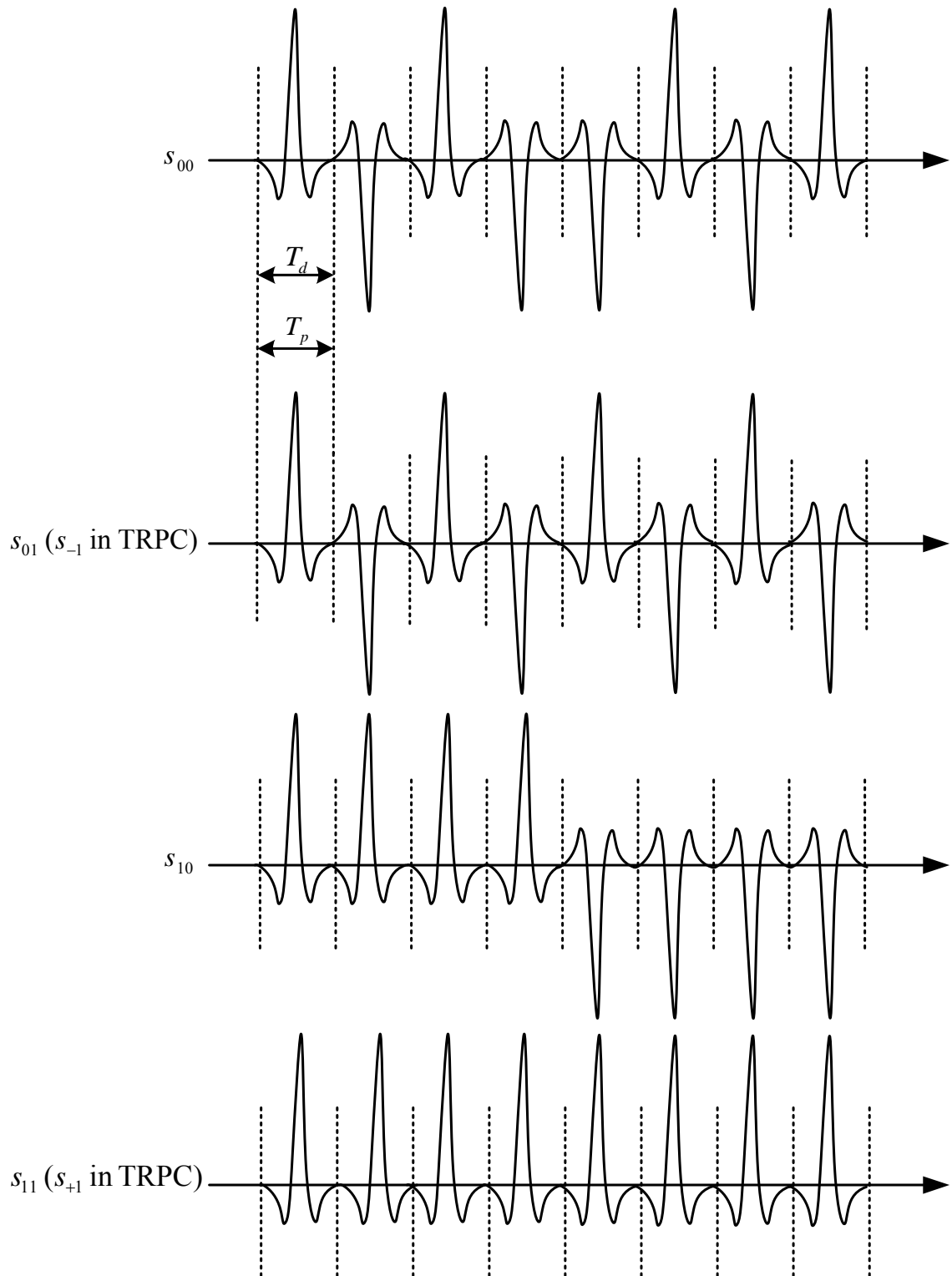
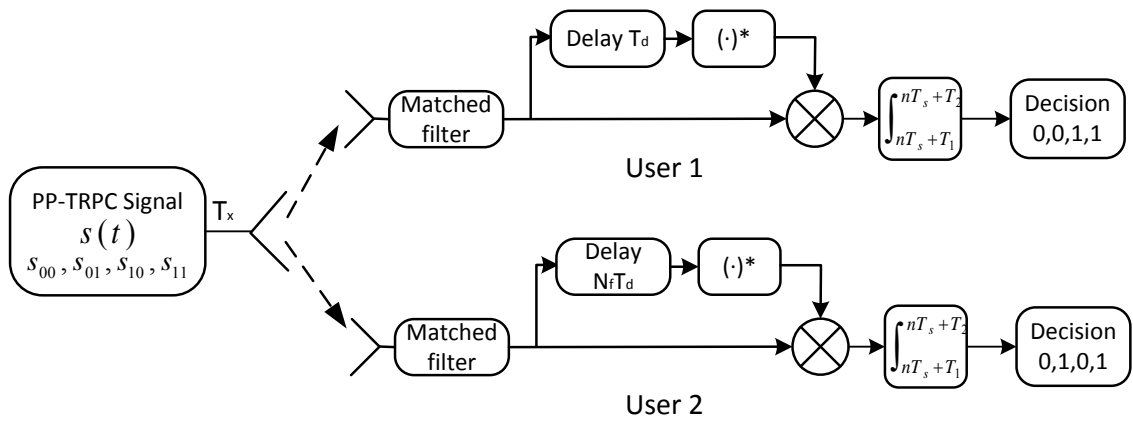Figure 4.1: PP-TRPC pulse pattern structure ($N_f = 4$)

Figure 4.2: PP-TRPC zero threshold decision receiver structure

4.2. After the autocorrelation receiver, the decision variable for user 1 is D_1 and for user 2 it is D_2. Then D_1 and D_2 are compared with zero to make decisions.

$$D_1 = \int_{nT_s+T_1}^{nT_s+T_2} r(t)r^*(t-T_d)\mathrm{d}t$$

$$D_2 = \int_{nT_s+T_1}^{nT_s+T_2} r(t)r^*(t-N_fT_d)\mathrm{d}t$$

(4.6)

If the bits $\{s_{00}, s_{01}, s_{10}, s_{11}\}$ are transmitted without noise, the decoded bits should be $\{0, 0, 1, 1\}$ at user 1 and $\{0, 1, 0, 1\}$ at user 2. In this way, the transmitter can communicate with two users simultaneously. So the overall bit rate of PP-TRPC is doubled compared with original TRPC while using the same amount of transmitting energy. According to [16] and [21], $\mathrm{Re}\{D_1\}$ and $\mathrm{Re}\{D_2\}$ can be approximated as Gaussian random variables. Similar to the analysis in [16], we can estimate the mean of $\mathrm{Re}\{D_1\}$ as follows

$$E[\mathrm{Re}\{D_1\}]\Big|_{s_{00}} \approx \frac{E_b}{2N_f}\left[-(2N_f-3)E_pE_h + \sum_{l=L_1}^{L_2}\sum_{\substack{k=L_1\\k\neq l}}^{L_2}\mathrm{Re}\{\alpha_l\alpha_k^*\}\times R_{ss}(|T_d-\tau_l+\tau_k|)\right]$$

$$E[\mathrm{Re}\{D_1\}]\Big|_{s_{01}} \approx \frac{E_b}{2N_f}\left[-(2N_f-1)E_pE_h + \sum_{l=L_1}^{L_2}\sum_{\substack{k=L_1\\k\neq l}}^{L_2}\mathrm{Re}\{\alpha_l\alpha_k^*\}\times R_{ss}(|T_d-\tau_l+\tau_k|)\right]$$

$$E[\mathrm{Re}\{D_1\}]\Big|_{s_{10}} \approx \frac{E_b}{2N_f}\left[(2N_f-3)E_pE_h + \sum_{l=L_1}^{L_2}\sum_{\substack{k=L_1\\k\neq l}}^{L_2}\mathrm{Re}\{\alpha_l\alpha_k^*\}\times R_{ss}(|T_d-\tau_l+\tau_k|)\right]$$

$$E[\mathrm{Re}\{D_1\}]\Big|_{s_{11}} \approx \frac{E_b}{2N_f}\left[(2N_f-1)E_pE_h + \sum_{l=L_1}^{L_2}\sum_{\substack{k=L_1\\k\neq l}}^{L_2}\mathrm{Re}\{\alpha_l\alpha_k^*\}\times R_{ss}(|T_d-\tau_l+\tau_k|)\right]$$

(4.7)

where E_p is the energy of a single pulse $p(t)$, which is the convolution result of transmitted pulse $p_{tr}(t)$ and receiver matched filter. $E_h = \sum_{k=K_1}^{K_2} |\alpha_k|^2$. L_1 and L_2 correspond to the integration interval $[T_1, T_2]$. $R_{ss} = \int_{-\infty}^{\infty} s(t)s(t+\tau)\mathrm{d}t$.

Similarly, we have the mean of $\mathrm{Re}\{D_2\}$

$$E[\mathrm{Re}\{D_2\}] \approx \frac{E_b}{2N_f}\left[N_{b_m}E_pE_h + \sum_{l=L_1}^{L_2}\sum_{\substack{k=L_1\\k\neq l}}^{L_2}\mathrm{Re}\{\alpha_l\alpha_k^*\} \times R_{ss}(|N_fT_d - \tau_l + \tau_k|)\right] \quad (4.8)$$

where N_{b_m} is given by

$$N_{b_m} = \begin{cases} -N_f, & b_m = 00 \text{ or } 10 \\ N_f, & b_m = 01 \text{ or } 11 \end{cases} \quad (4.9)$$

In order to get the BER performance of PP-TRPC, the variance of $\mathrm{Re}\{D_1\}$ is calculated similar to [16]

$$\begin{aligned}
\mathrm{Var}[\mathrm{Re}\{D_1\}] = &\frac{E_bN_0}{4N_f}\int_{T_1}^{T_2}\int_{T_1}^{T_2}\mathrm{Re}\{q_{b_m}(t)q_{b_m}^*(t')\} \times R_{tr}(t'-t)\mathrm{d}t\mathrm{d}t' \\
&+ \frac{E_bN_0}{4N_f}\int_{T_1}^{T_2}\int_{T_1}^{T_2}\mathrm{Re}\{q_{b_m}(t-T_d)q_{b_m}^*(t'-T_d)\} \times R_{tr}(t'-t)\mathrm{d}t\mathrm{d}t' \\
&+ \frac{E_bN_0}{4N_f}\int_{T_1}^{T_2}\int_{T_1}^{T_2}\mathrm{Re}\{q_{b_m}(t)q_{b_m}^*(t'-T_d)\} \times R_{tr}(t'-t+T_d)\mathrm{d}t\mathrm{d}t' \\
&+ \frac{N_0^2}{2}\int_{-(T_2-T_1)/\sqrt{2}}^{(T_2-T_1)/\sqrt{2}}(\sqrt{2}(T_2-T_1)-2|t|)R_{tr}^2(\sqrt{2}t)\mathrm{d}t
\end{aligned} \quad (4.10)$$

where $b_m \in \{00, 01, 10, 11\}$ and $R_{tr}(\tau) = \int_{-\infty}^{\infty} p_{tr}(t)p_{tr}(t-\tau)\mathrm{d}t$.

Similarly, replacing T_d in (4.10) by N_fT_d, we can get the variance of $\mathrm{Re}\{D_2\}$. So

the overall probability of error for the two users ZDT PP-TRPC system is

$$Pe = \frac{1}{8} \sum_{i=1}^{2} \sum_{b_m \in \{00,01,10,11\}} \left[Q \left(\frac{S_{i,b_m} E[\mathrm{Re}\{D_i\}]|_{s_{b_m}}}{\sqrt{\mathrm{Var}[\mathrm{Re}\{D_i\}]|_{s_{b_m}}}} \right) \right] \qquad (4.11)$$

where S_{i,b_m} is the sign of the bit for the ith user when s_{b_m} is transmitted. It is given by

$$S_{1,b_m} = \begin{cases} -1, & b_m = 00 \\ -1, & b_m = 01 \\ +1, & b_m = 10 \\ +1, & b_m = 11 \end{cases} \qquad S_{2,b_m} = \begin{cases} -1, & b_m = 00 \\ +1, & b_m = 01 \\ -1, & b_m = 10 \\ +1, & b_m = 11 \end{cases} \qquad (4.12)$$

In order to further improve the BER performance of PP-TRPC, we can utilize adaptive threshold decision. First, a training sequence with $4N_t$ symbols is sent before the data packet. The ADT PP-TRPC receiver structure is shown in Fig. 4.3. Because of the asymmetry of D, two ADTs are needed for each $D_i, i \in \{1, 2\}$. These ADTs can be denoted as $\xi_{i,m}, m \in \{0, 1\}$, which represents the threshold for D_i when the decision for $D_j (j \neq i)$ is m. They can be calculated utilizing the training sequence,

$$\begin{aligned} \xi_{1,m} &= \frac{1}{2N_t} \sum_{k=0}^{N_t-1} (D_{1,4k+m+1} + D_{1,4k+m+3}) \\ \xi_{2,m} &= \frac{1}{2N_t} \sum_{k=0}^{N_t-1} (D_{2,4k+2m+1} + D_{2,4k+2m+2}) \end{aligned} \qquad (4.13)$$
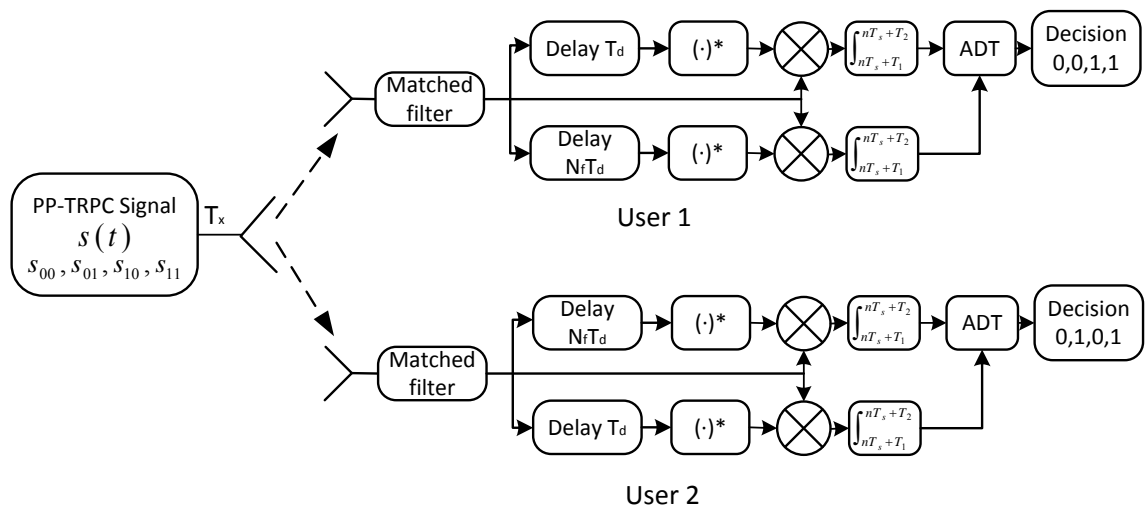
where $m \in \{0, 1\}$.

Figure 4.3: PP-TRPC adaptive decision threshold receiver structure

In the basic decision strategy, the ith user will get $D_j (j \neq i)$ first. Based on the result of D_j, the ith user will choose a corresponding ADT to make decision for D_i. Because of the difference in the conditional thresholds, a wrong decision on D_j will result in a wrong threshold. To reduce this kind of error, we can implement an improved decision strategy, which is illustrated in Fig. 4.4. In the ideal situation, all the ξ are chosen correctly, the overall probability of error for the two users ADT PP-TRPC system is

$$Pe = \frac{1}{8} \sum_{i=1}^{2} \sum_{b_m \in \{00,01,10,11\}} \left[Q \left(\frac{S_{i,b_m} (E[\text{Re}\{D_i\}]|_{s_{b_m}} - \xi_{i,m})}{\sqrt{\text{Var}[\text{Re}\{D_i\}]|_{s_{b_m}}}} \right) \right] \quad (4.14)$$

where S_{i,b_m} is the same as in (4.12).

In reality, the number of users can be a lot more than two. In order to support more users in PP-TRPC, we need more pulse patterns. A straightforward implementation is to increase the pulse numbers in $\{s_{00}, s_{01}, s_{10}, s_{11}\}$. For example, in the 4 users scenario, we can denote $s_{000} = [s_{00}, 0000, -s_{00}]$, $s_{001} = [s_{00}, 0000, s_{00}]$, each of which contains 16 pulses. We can use D_3 to separate 4 users into 2 groups. D_1 and D_2 are used to make decisions within each group, which is the same as in the 2 users case. D_1, D_2 and D_3 are given as follows,

$$D_1 = \int_{nT_s+T_1}^{nT_s+T_2} r(t)r^*(t - T_d)\mathrm{d}t$$
$$D_2 = \int_{nT_s+T_1}^{nT_s+T_2} r(t)r^*(t - 4T_d)\mathrm{d}t \quad (4.15)$$
$$D_3 = \int_{nT_s+T_1}^{nT_s+T_2} r(t)r^*(t - 12T_d)\mathrm{d}t$$

This scheme requires 16 pulses to compose each symbol. So the energy needed
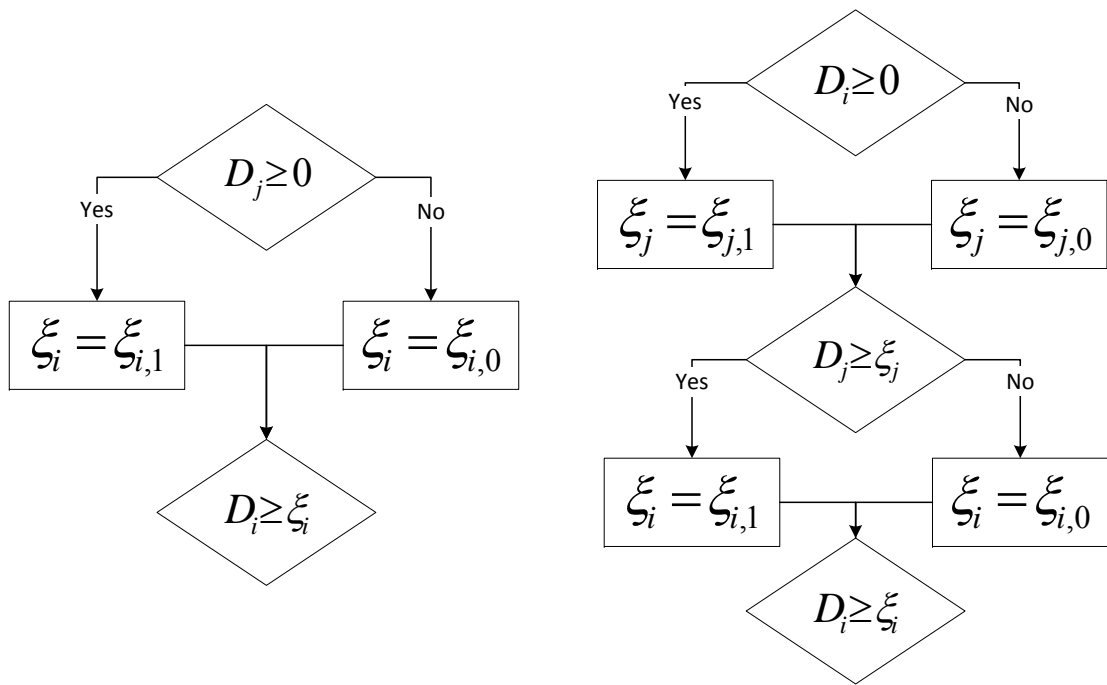
Figure 4.4: ADT PP-TRPC basic and improved decision strategy

to send same amount of bits is doubled compared with 2 users case, which is a major disadvantage for the low power UWB system. In addition, the autocorrelation receiver for D_3 requires a delay line with length of $12T_d$. This will greatly increase the implementation complexity for this system. To solve these problems, we can reduce the pulse numbers to 8 in each symbol. For instance, the symbol s_{000} can be simplified as $[+1, -1, -1, +1, 0, 0, -1, +1, +1, -1]$. This simplified scheme uses half the energy in the 16 pulses scheme to transmit each bit. Moreover, the longest delay line needed in the simplified scheme is $6T_d$. The detailed simplified pulse patterns are illustrated in Fig. 4.5.

4.2 Numerical and Simulation Results

We first show the numerical and simulation results for 2 users PP-TRPC scheme. The pulse length is $T_p = 2.02$ ns and each pulse cluster consists of 8 consecutive pulses. The symbol duration is $T_s = 250$ ns, which is longer than the delay spread of all CM1 channels and most CM8 channels. So there will be no ISI for CM1 and very little ISI for CM8. The numerical results for ZDT and ADT are calculated with (4.11) and (4.14) respectively. The numerical and simulation results are both averaged over 100 channels. For simulations using ADT, the improved decision strategy is adopted. Fig. 4.6 and Fig. 4.7 present the comparison between numerical and simulation results in CM1 and CM8. We can see that these two types of results match very well, which indicates the effectiveness of our numerical analysis. In addition, there is a 3 dB performance gap at BER=10^{-3} introduced by ADT for CM1. This improvement is even greater at lower BER, which means the additional complexity of ADT is
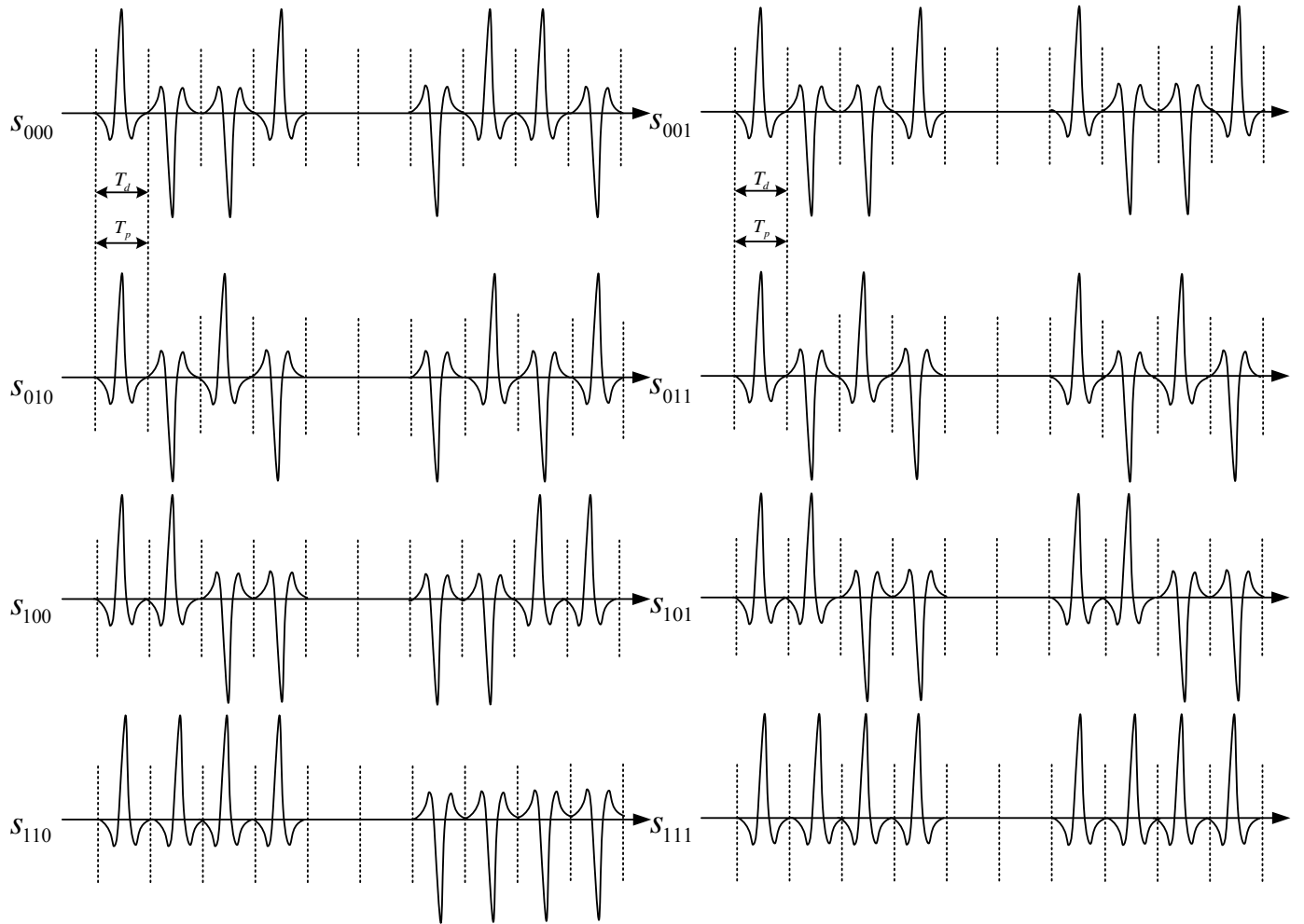
Figure 4.5: Simplified PP-TRPC pulse patterns for 4 users

worthwhile for strong LOS channels. However, the gap is less than 1 dB for CM8 at BER=10^{-3}. And it remains at 1 dB for BER=10^{-5}. So for CM8 which represents NLOS with a large delay spread, the extra complexity of ADT is optional. In this case, we can just implement ZDT receivers with lower cost and still achieve acceptable performance.

Fig. 4.8 shows the BER performance of PP-TRPC (4 users) using 8 pulses and 16 pulses schemes. In addition to lower complexity, 8 pulses scheme also outperform 16 pulses scheme by a significant gap. At BER $= 10^{-3}$, the performance gap is 2.5 dB and 1.7 dB in CM1 and CM8 channels respectively. In the following results, we will only consider 8 pulses scheme for PP-TRPC (4 users). We can also see that the BER performance of CM8 outperforms that of CM1 at SNR $= 20$ dB. PP-TRPC has much larger IPI than conventional TRPC, which is the main reason of performance degradation at high SNR. For the CIR of CM1, the largest tap and the second largest one are usually packed closely together. While in CM8, the relative large taps are spread over a larger range. This results in smaller IPI which accounts for the major part of MUI at high SNR.

For a fair comparison, the overall bit rate of PP-TRPC and TD-TRPC are set to be the same. In 2 users and 4 users case, the bit rate for both schemes is 8 Mbps. So the symbol duration of TD-TRPC is $T_s = 125$ ns. This symbol duration is the same for both the 2 users and 4 users case. So the BER performance of the 2 users and 4 users case is the same for TD-TRPC. The BER performance comparison of PP-TRPC and TD-TRPC is shown in Fig. 4.9 with CM1 channels. It is found that PP-TRPC (2 users) and PP-TRPC (4 users) outperform TD-TRPC by 1.2 dB and 1.8 dB at BER $= 10^{-3}$. But this performance gap is smaller at higher SNR. Because the symbol

duration of TD-TRPC is larger than the delay spread of most CM1 channels. The ISI of TD-TRPC can be neglected in CM1 channels. So this performance improvement is mainly due to the energy reduction of PP-TRPC. We can also see from Fig. 4.9 that the 4 users case performs better than the 2 users at low SNR. This is expected because of the two empty pulse slots which can reduce the impact of IPI. However, there are 16 total pulse patterns with 4 users, which is double the size with 2 users. As a result, the difference between different decision thresholds is smaller for the 4 users case. This factor outweighs the IPI at high SNR. So the 2 users case outperforms the 4 users when SNR > 19 dB.

Fig. 4.10 shows the BER performance comparison in CM8 channels. The symbol duration of TD-TRPC $T_s = 125$ ns is shorter than the delay spread of most CM8 channels. However, PP-TRPC still have a symbol duration $T_s = 250$ ns. So TD-TRPC will perform much worse than PP-TRPC due to ISI. We can see from Fig. 4.10, PP-TRPC (2 users) and PP-TRPC (4 users) outperform TD-TRPC by 2 dB and 2.8 dB at BER $= 10^{-3}$ respectively. As we can expect, the performance improvement will become larger if we increase the bit rate.

Illustrated in Fig. 4.11 is a comparison between time division PP-TRPC and TD-TRPC with 16 users. Here PP-TRPC is based on the 8 pulses scheme for 4 users and there are 4 chip intervals within each symbol duration. So it can support a total of 16 users. Time division PP-TRPC outperforms TD-TRPC by 1.8 dB in both CM1 and CM8 channels at BER $= 10^{-3}$. At higher SNR, the performance gain becomes larger in CM8 channels but smaller in CM1 channels. This means that time division PP-TRPC is especially effective against NLOS and long delay spread of multipath channels.

4.3   Summary

In this chapter, a new scheme with different pulse patterns has been proposed to meet the needs of multiuser scenarios. We have obtained the numerical results of PP-TRPC with 2 users and showed its performance improvement over TD-TRPC. In addition, we have compared 8 and 16 pulses schemes in PP-TRPC with 4 users. Since 8 pulses scheme has better performance and lower complexity, it is our choice for multiple user PP-TRPC. We have also showed the performance of time division PP-TRPC by combining PP-TRPC and TD-TRPC. It yields very good performance in both LOS and NLOS channels and can be easily expanded to support more users as well.
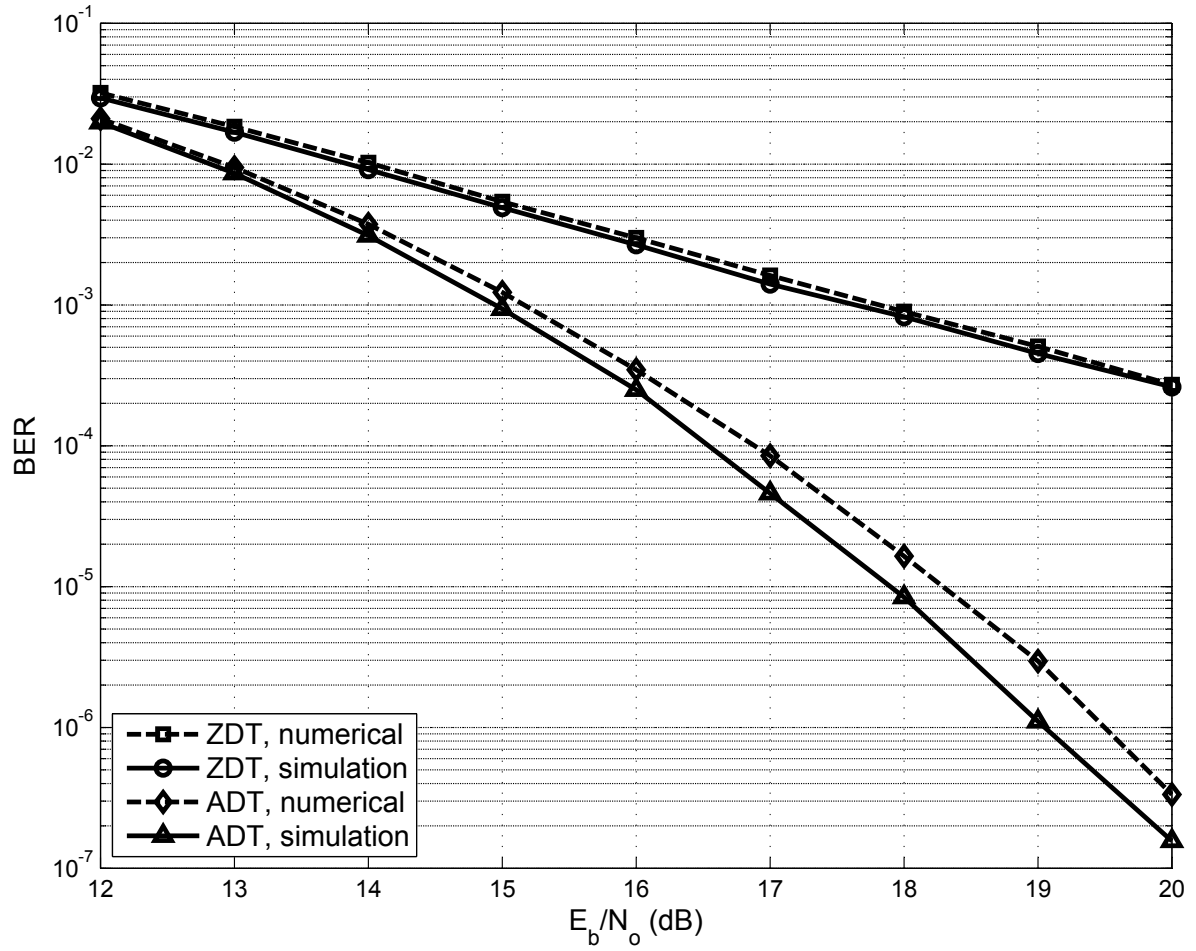
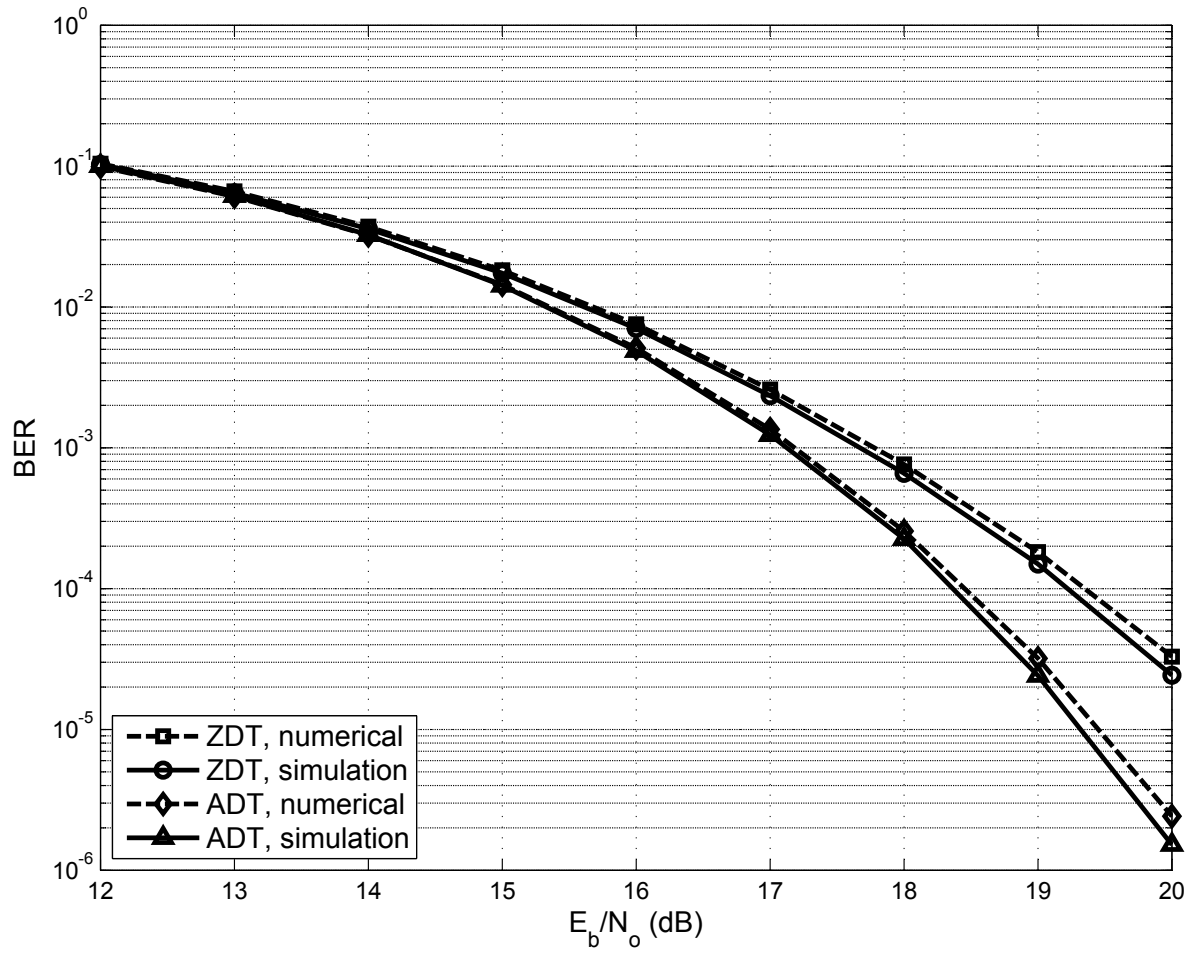Figure 4.6: BER of PP-TRPC with 2 users in CM1 channels

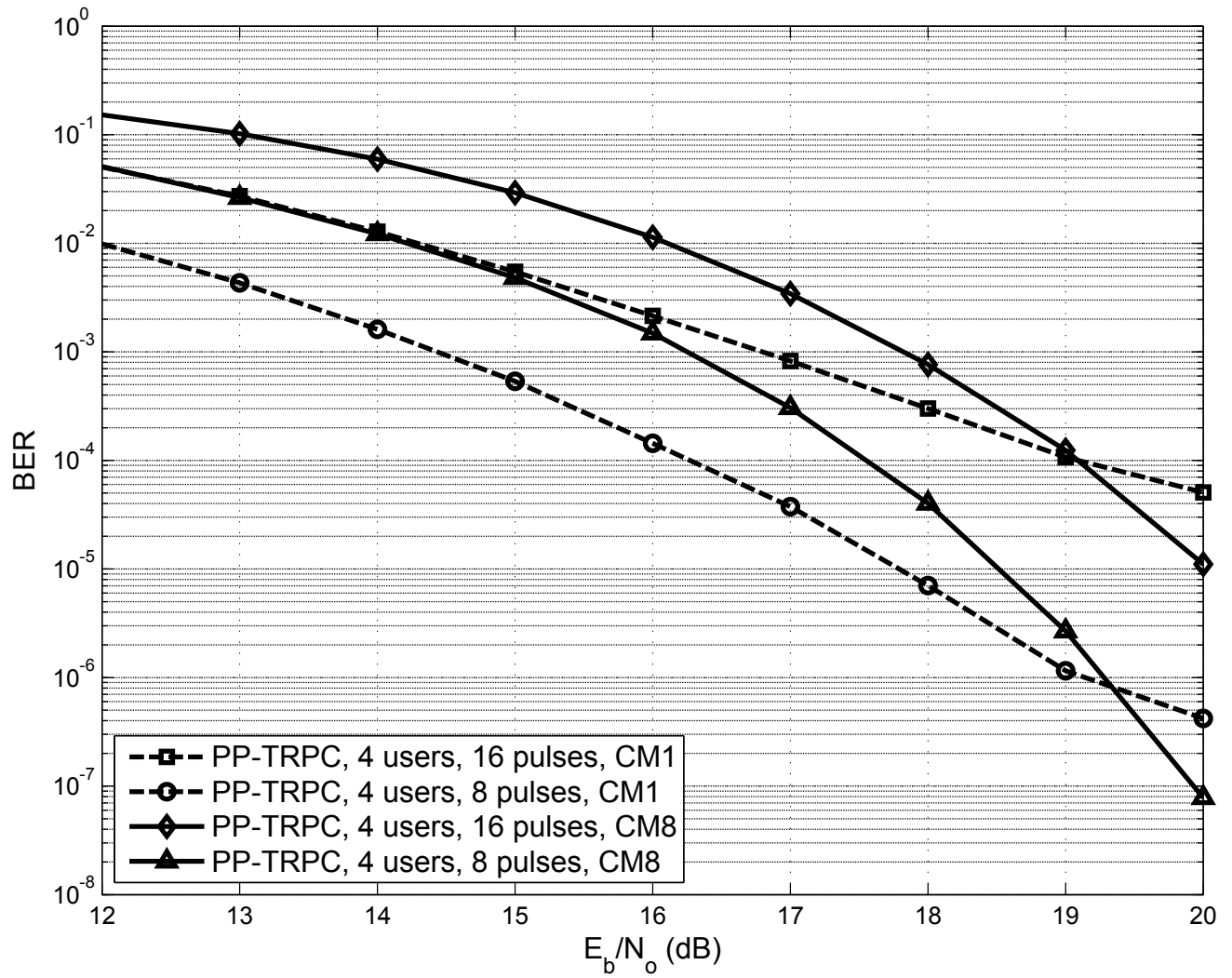Figure 4.7: BER of PP-TRPC with 2 users in CM8 channels

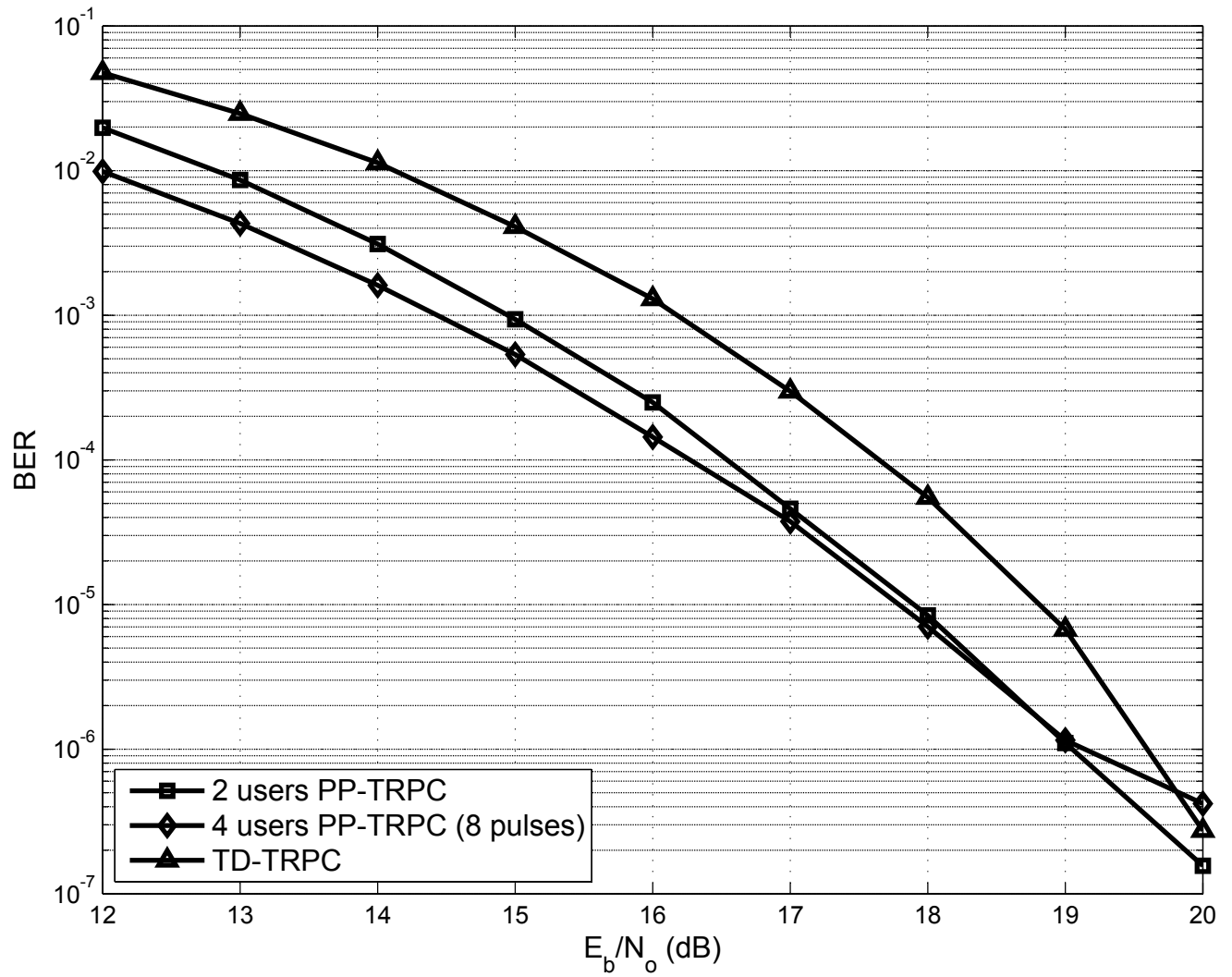Figure 4.8: BER of PP-TRPC (4 users) using 8 pulses and 16 pulses schemes

Figure 4.9: Simulation results of PP-TRPC and TD-TRPC in CM1 channels
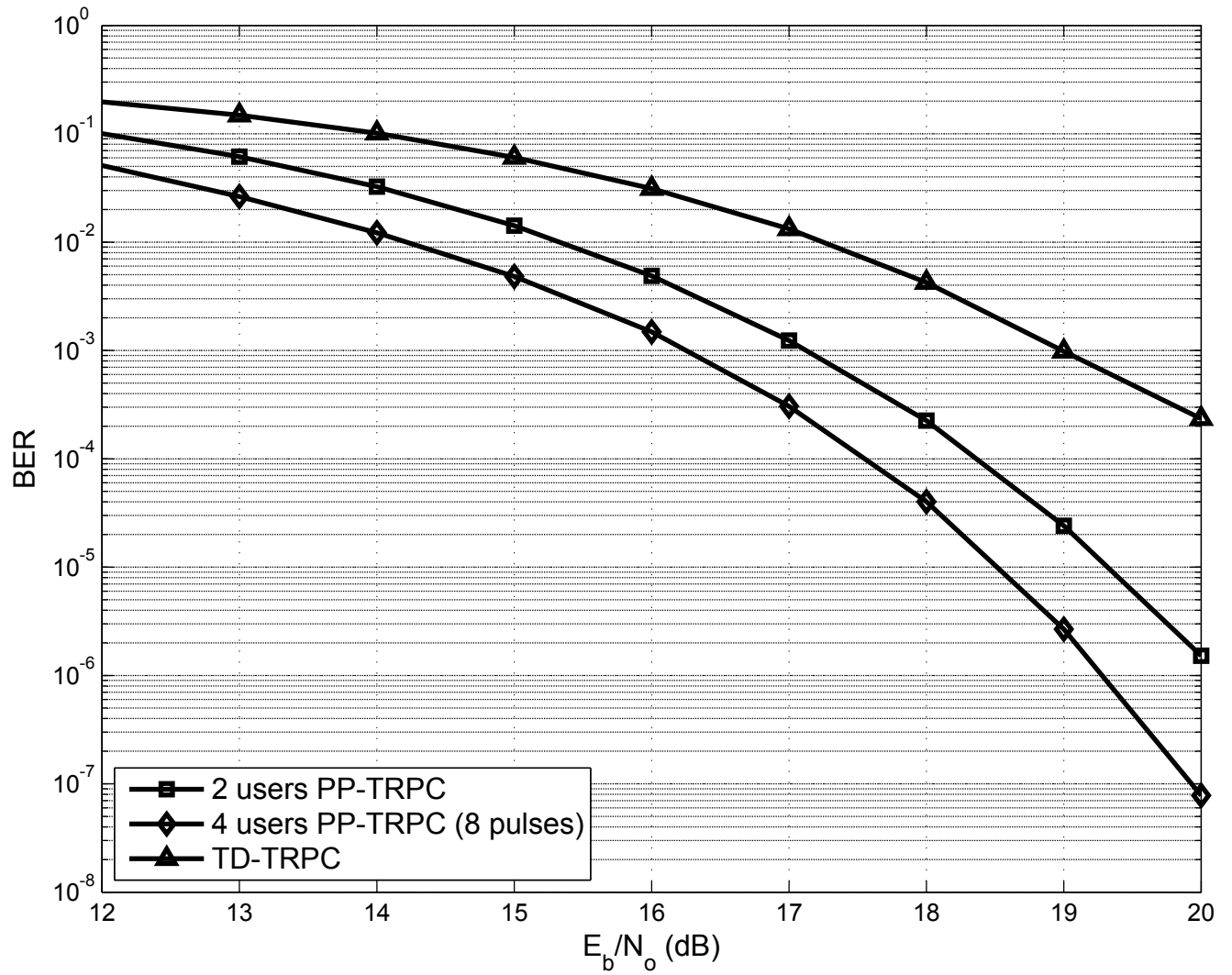
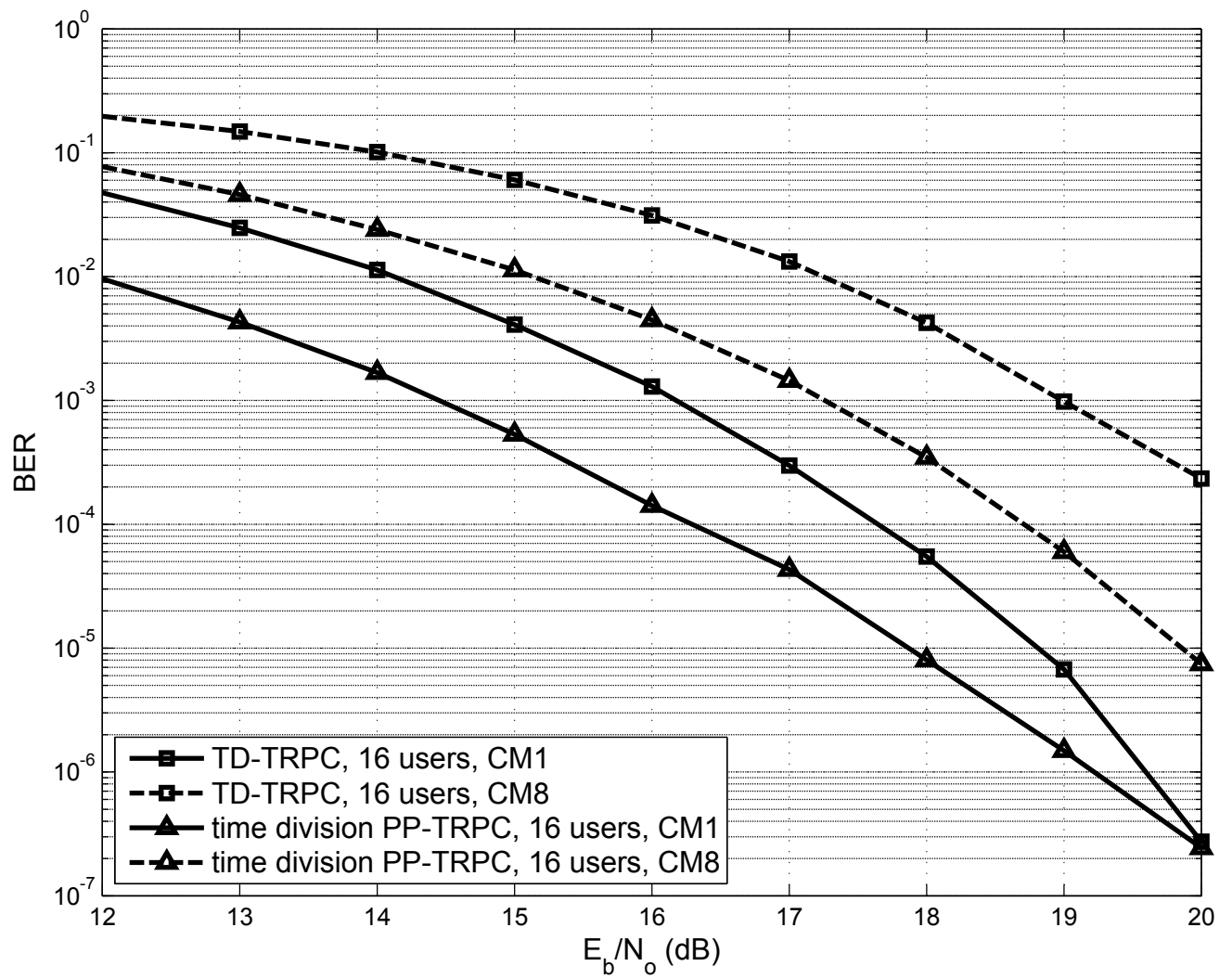Figure 4.10: Simulation results of PP-TRPC and TD-TRPC in CM8 channels

Figure 4.11: Simulation results of time division PP-TRPC and TD-TRPC with 16 users in both CM1 and CM8 channels

Chapter 5

Conclusion and Future Work

5.1 Conclusions

UWB technology has many advantages over conventional narrowband and other alternative systems, including low implementation complexity, low power consumption and great time resolution. However, conventional UWB systems need to implement long analog delay lines which is not feasible. TRPC was proposed to address this problem. The delay between data and reference pulses is only the pulse width and thus only pulse width delay lines are needed in the transmitter and receiver. Meanwhile, because of the short delay, IPI will be introduced. To further improve the performance of TRPC systems, we have proposed several multi-antenna receiver and transmitter schemes in this thesis.

The proposed multi-antenna receiver diversity schemes include EGC and different selection combining criteria. In a 1-by-2 system, EGC and selection based on DV, NCQI, LLR and SLLR significantly outperform selection based on channel length,

received energy and average received power. Among the better performed candidates, the performance of SLLR is slightly better than EGC, DV, NCQI and LLR. At the same time, SLLR selection is also easier to implement. So it would be the best candidate for a 1-by-2 system. But in a system with more than 2 receiver antennas, EGC achieves a significant performance gain over all the selection criteria. So in terms of BER performance, EGC is the best choice for more than 2 receiver antennas. Since EGC requires the processing of all the received branches, it will result in extra power consumption compared with selection combining. Hence receiver antenna selection still remains a viable choice for low power receiver designs.

For multi-antenna transmitter diversity schemes, we have studied direct sum, delay diversity and antenna selection diversity. Among them, antenna selection shows much better performance. In addition, SCQI outperforms all the other selection criteria in terms of BER performance and implementation complexity. We have also considered the case of 2-by-2 system, the overall choice would be receiver antenna selection based on SLLR and transmitter antenna selection based on SCQI.

We have also proposed a new multi-user downlink scheme named as PP-TRPC. By changing the pulse patterns for 2 and 4 users, the overall bit rate is increased which can improve the BER performance. Unlike TD-TRPC, it can also keep the same frame duration as TRPC without introducing ISI. As the simulation and numerical results suggest, PP-TRPC has significant better performance than TD-TRPC. However, this comes with the cost of higher complexity. For a system with more than 4 users, we have shown the performance of time division PP-TRPC which combines PP-TRPC and TD-TPRC. It performs well in both LOS and NLOS channels and can be easily expanded to support more users as well.

5.2   Future Work

Although the results presented in this thesis have demonstrated the effectiveness of receiver and transmitter diversity for TRPC as well as the performance gain of PP-TRPC for downlink multi-user scenario, they could be further developed in a few ways:

1. The results of this thesis are based on the IEEE 802.15.4a channel models. They are all LOS (CM1) or NLOS (CM8) for all antennas, but in reality, the channel conditions can be much more complex. LOS and NLOS channels can exist at the same time for different antennas. The diversity schemes should be studied for all kinds of channel models or even measured channels. In addition, the interference between different antennas is ignored here which may not be the case in reality. So the interference mitigation techniques should be studied as well.

2. For receiver diversity, although MRC can not be applied to TRPC, we can implement a weighted combining by assigning different weights for different receiver antennas which will probably outperform EGC.

3. For the PP-TRPC schemes proposed in Chapter 4, it can be expanded to both uplink and downlink. For example, each user can be assigned a unique pulse pattern and use it for transmitting and receiving. It can even be combined with antenna diversity discussed in Chapter 2 and 3 by implementing multiple antenna at each user.

Bibliography

[1] J. Reed. An introduction to ultra wideband communication systems. *Prentice Hall PTR*, 2005.

[2] T. W. Barrett. History of ultrawideband (uwb) radar & communications: Pioneers and innovators. *Progress In Electromagnetics Symposium*, 2000.

[3] R. A. Scholtz. Multiple access with time-hopping impulse modulation. *IEEE MILCOM*, 2:447–450, October 1993.

[4] T. E. McEwan. Ultra-wideband radar motion sensor. *U.S. Patent 5,361,070, issued November 1, 1994*, 1994.

[5] R. S. Kshetrimayum. An introduction to uwb communication systems. *Potentials, IEEE*, 28(2):9–13, March 2009.

[6] Federal Communications Commission. Revision of part 15 of the commission's rules regarding ultra-wideband transmission systems. *First note and Order*, February 2002.

[7] J. Iinatti I. Oppermann, M. Hamalainen. Uwb theory and applications. *John Wiley & Sons Ltd*, 2004.

[8] R. J. Fontana. A brief history of uwb communications. *Multispectral Solutions Inc., Kluwer Academic/Plenum Publishers*, 2000.

[9] R. J. Fontana. Recent system applications of short-pulse uwb technology. *IEEE Trans on Microwave Theory and Techniques*, 52:2087–2104, September 2004.

[10] E. Karapistoli, F.-N. Pavlidou, I. Gragopoulos, and I. Tsetsinas. An overview of the ieee 802.15.4a standard. *Communications Magazine, IEEE*, 48(1):47–53, January 2010.

[11] A. F. Molisch, K. Balakrishnan, C.-C. Cassioli, D.and Chong, S. Emami, A. Fort, J. Karedal, J. Kunisch, H. Schantz, U. Schuster, et al. Ieee 802.15. 4a channel model-final report. *IEEE P802*, 15(04):0662, 2004.

[12] M. Z. Win, G. Chrisikos, and N. R. Sollenberger. Performance of rake reception in dense multipath channels: implications of spreading bandwidth and selection diversity order. *Selected Areas in Communications, IEEE Journal on*, 18(8):1516–1525, Aug 2000.

[13] B. L. Basore. Noise-like signals and their detection by correlation. Technical report, DTIC Document, 1952.

[14] M. R. Casu and G. Durisi. Implementation aspects of a transmitted-reference uwb receiver. *Wireless Communications and Mobile Computing*, 5(5):537–549, 2005.

[15] X. Dong, A. C. Lee, and L. Xiao. A new uwb dual pulse transmission and detection technique. In *ICC*, pages 2835–2839, 2005.

[16] X. Dong, L. Jin, and P. Orlik. A new transmitted reference pulse cluster system for UWB communications. *Vehicular Technology, IEEE Transactions on*, 57(5):3217–3224, 2008.

[17] X. Dong and L. Jin. Adaptive threshold for tr pulse cluster systems. In *Radio and Wireless Symposium, 2007 IEEE*, pages 109–112. IEEE, 2007.

[18] S. Zhou, G.B. Giannakis, and C. L. Martret. Chip-interleaved block-spread code division multiple access. *Communications, IEEE Transactions on*, 50(2):235–248, Feb 2002.

[19] L. Jin and X. Dong. Multiple access transmitted reference pulse cluster system for uwb communications. In *Electrical and Computer Engineering, 2007. CCECE 2007. Canadian Conference on*, pages 1333–1336. IEEE, 2007.

[20] Q. Zhang and C. Sum Ng. Differentially-encoded di-symbol time-division multiuser impulse radio in uwb channel. *Communications, IEEE Transactions on*, 56(4):608–618, April 2008.

[21] X. Dong, L. Xiao, and A. C. Y. Lee. Performance analysis of dual pulse transmission in UWB channels. *IEEE Commun. Lett.*, 10(8):626–628, 2006.